#3

NONLINEAR PROPERTIES OF FM LIMITERS

LUIZ C. BAHIANA

TECHNICAL REPORT 350

MAY 29, 1959

MASSACHUSETTS INSTITUTE OF TECHNOLOGY
RESEARCH LABORATORY OF ELECTRONICS
CAMBRIDGE, MASSACHUSETTS

The Research Laboratory of Electronics is an interdepartmental laboratory of the Department of Electrical Engineering and the Department of Physics.

The research reported in this document was made possible in part by support extended the Massachusetts Institute of Technology, Research Laboratory of Electronics, jointly by the U. S. Army (Signal Corps), the U. S. Navy (Office of Naval Research), and the U. S. Air Force (Office of Scientific Research, Air Research and Development Command), under Signal Corps Contract DA36-039-sc-78108, Department of the Army Task 3-99-20-001 and Project 3-99-00-000.

MASSACHUSETTS INSTITUTE OF TECHNOLOGY

RESEARCH LABORATORY OF ELECTRONICS

Technical Report 350 May 29, 1959

NONLINEAR PROPERTIES OF FM LIMITERS

Luiz C. Bahiana

This report is based on a thesis submitted to the Department of Electrical Engineering, M.I.T., January 20, 1958, in partial fulfillment of the requirements for the degree of Master of Science.

Abstract

A resistive model for the double-diode amplitude limiter is used in an investigation of the characteristics of a double-diode tuned limiter. It is assumed that the tuned circuit can be replaced by an equivalent resistance (equal to the impedance of the tuned circuit at the given driving frequency). The crystal diodes are assumed to follow a square-law volt-ampere dependence when they are conducting. A limiter coefficient K_L is suggested and shown to be a convenient parameter for defining the limiter performance. The characteristics calculated on the basis of this theory agree, within a reasonable degree of approximation, with available experimental data. To solve the limiter problem with the tuned circuit shunted by ideal diodes, a breakpoint analysis that results in a set of transcendental equations, called the limiter equations, is carried out. In view of the complexity of such equations, a numerical solution is worked out. Subsequent correlation shows that the resistive model is a good approximation for amplitudes, but cannot account for a variation of phase with amplitude that is indicated by the solution of the limiter equations. A revised model is suggested to take care of the phase distortion. The predictions of this model are shown to be qualitatively correct. Further research in this general field is suggested.

TABLE OF CONTENTS

I. INTRODUCTION

This research work constitutes an investigation of the characteristics and performance of FM amplitude limiters. The operation of such limiters depends upon the interaction between nonlinear elements and energy-storage elements. A rigorous mathematical analysis of these circuits generally becomes exceedingly involved, but approximate solutions can be found by the use of suitable simplifying assumptions.

Among other problems, the effect of bias on the damping effects of diodes and the dependence of the conduction period on the circuit parameters are outstanding. Two of the assumptions that have usually been made are that the conduction period is very small (so that the diodes conduct by pulses), and that the voltage across a tuned circuit loaded by diodes is very nearly sinusoidal.

We shall avoid these assumptions and assume, instead, that the tuned circuit does not upset the conduction period of diodes, and hence the waveforms are nonsinusoidal. This will enable us to calculate the fundamental component of the output voltage by Fourier methods. Our assumption is embodied in a model (referred to here as the "resistive model") in which the tuned circuit is replaced by an equivalent resistance (see sec. 2.2).

This assumption seems to be validated by practice. Results of measurements by Paananen (1) on a 60-cps resistive model and on a 28-mc limiter circuit bear this out. The operation of crystal limiters at 184-mc was studied by Brandeau (2), and his results agree with Paananen's. Shapiro (3) measured the characteristics of a biased limiter, and the differences between low-frequency resistive operation and high-frequency operation with the use of a tuned circuit were not found significant.

We shall attempt to use the results of our analysis as the elementary background for limiter design. As Paananen (4) points out: "the literature on limiters is very meager and most of the emphasis is given to qualitative, or semi-quantitative treatment of grid-leak limiters. One outstanding deficiency is the lack of parameters to describe limiting performance, such as exist abundantly for evaluation of linear amplifier performance."

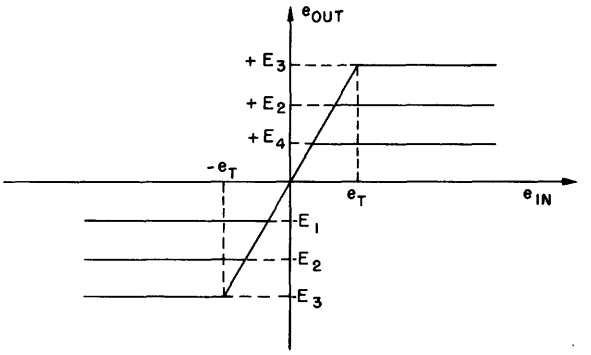

Fig. 1. Characteristics of an idealized clipper.

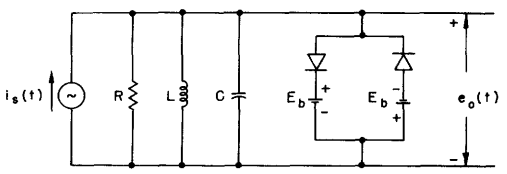

Fig. 2. Double-diode biased limiter.

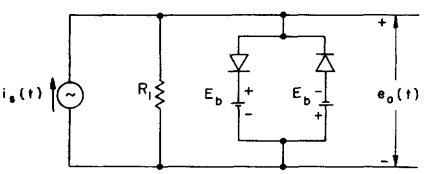

Fig. 3. Resistive model (ideal diodes).

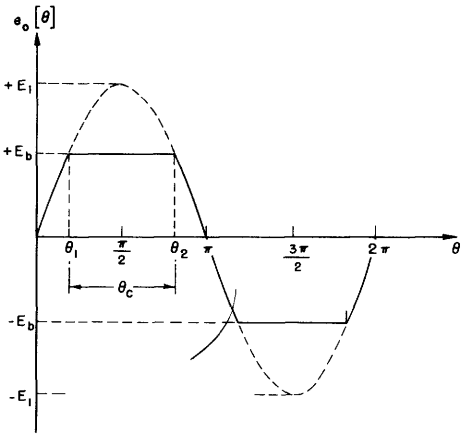

Fig. 4. Voltage across biased limiter (sinusoidal input).

II. THE RESISTIVE MODEL FOR DIODE-LIMITER ANALYSIS

2.1 FUNDAMENTAL ASSUMPTIONS AND DEFINITIONS

Amplitude limiting can be defined as the process whereby the amplitude of a wave is clamped at a predetermined value. Any device in which amplitude limiting is achieved is called an "amplitude limiter," or simply "limiter."

2.11 The Ideal Limiter Concept

The operations of clipping and limiting are closely related, but there is a fundamental difference between them. Clipping is a static process. In a clipper the instantaneous value of a wave is prevented from exceeding a predetermined value. The curves of Fig. 1 represent the characteristics of an idealized clipper, if e_{in} and e_{out} are instantaneous values. The output of a clipper is a flat-topped wave of constant amplitude. Limiting, on the other hand, is a dynamic process. An ideal limiter is a device whose input is a sine wave of variable amplitude and arbitrary frequency and whose output is a sine wave of fixed amplitude and the same frequency. In Fig. 1, the curves lying in the first quadrant represent an idealized limiter characteristic, if e_{in} and e_{out} are sinusoidal amplitudes. A truly ideal limiter would have no threshold (called e_T in Fig. 1), and so the output amplitude would remain constant for arbitrarily small input amplitudes. For such a limiter, characteristics are unnecessary; it would be completely characterized by its output amplitude. However, as would be expected, practical limiters are nonideal, and a set of characteristics is a convenient device for comparing the performance of a given limiter with the ideal limiter. However, it is not the only means, and, as we shall show presently, there are other factors to be taken into account when specifying the performance of a limiter.

2.12 Properties of Actual Limiters

In order to be able to investigate the performance of limiters, we shall establish three basic conditions that should be fulfilled as completely as possible:

(a) The fluctuations in the output amplitude should be kept to a minimum over the largest possible range of input amplitudes. The performance of a limiter in this respect will be described by the limiter coefficient, as defined in section 2.4.

(b) The limiting process should not fail when the input amplitude varies abruptly. A limiter that fulfills this condition is said to be rapid-acting.

(c) The limiter output should be as free of distortion as possible. The distortion we refer to here is the introduction of undesirable modifications in the message modulation of the input signal. Although this may become a problem in other applications, what we have in mind is the specific case of FM limiters. This point will be discussed in detail in Section VII.

Although there might be other desirable features for a limiter, the three basic conditions stated above, particularly condition (a), are of fundamental importance. We shall spend most of our time investigating under what conditions and to what extent these conditions are fulfilled in actual limiters.

2.13 The Double-Diode Limiter

Among several types of limiters that are now used, the double-diode limiter was chosen as the object of this investigation. At least two other types of limiter are equally important: the overdriven amplifier (5), and the gated-beam tube (4). The overdriven amplifier depends, for effective limiting, on the action of a capacitor in its grid circuit. The operation of this circuit is affected by the rate of change of the input amplitude. The gated-beam tube exhibits a considerable variation of parameters from tube to tube; this complicates the design of limiters that use such tubes.

The double-diode crystal limiter is very rapid-acting. The variations in the parameters of crystal diodes are negligible as far as the design of limiters is concerned. This accounts for the increasing popularity of diode limiters and amply justifies our choice.

Figure 2 shows a simplified model of a double-diode biased limiter. The parallel RLC circuit is a valid representation of the tank circuit found in practice, as shown in Section VI. The diodes are of the semiconductor type. The bias is given by batteries in series with the diodes, and the circuit is fed by a current source.

The actual solution for the limiter problem will be investigated in Section VI. In Sections III-V, a resistive model for the circuit of Fig. 2 will be considered.

2.2 RESISTIVE MODEL OF THE DIODE LIMITER

The assumption leading to the resistive model consists in admitting that we may neglect the effect of the tuned circuit on the diode. The tuned circuit is replaced by an equivalent resistance, equal in magnitude to the impedance of the tuned circuit at the frequency of operation. The fundamental component of the output voltage is then assumed to be, as a first approximation, equal to the output voltage of the actual limiter. Although this simplification seems to strip the problem of all its difficulties, we shall find that the resistive limiter presents several interesting properties. For one thing, the resistive model permits an investigation of the effects of nonideal diodes with a minimum of additional complication. Measurements of the characteristics of a resistive model have been carried out (4), so that the results of our theory can be conveniently checked. Moreover, the resistive model can be used as a building block for a more realistic analysis of the problem.

Figure 3 shows the resistive model of the double-diode biased limiter. The circuit is self-explanatory. Both ideal and nonideal diodes will be considered.

In section 2.3, ideal diodes will be assumed and the fundamental component of the output voltage will be computed. Nonideal diodes will be brought into the picture in Sections III and IV.

2.3 ANALYSIS OF THE RESISTIVE MODEL WITH IDEAL DIODES

The performance of the resistive model with ideal diodes will be investigated for a sinusoidal input of arbitrary frequency ω and constant amplitude. By ideal diodes, we mean diodes with zero forward resistance and infinite backward resistance. Let the input current be given by

$$i_s(t) = I_s \sin \omega t = I_s \sin \theta$$

The voltage across the limiter is in phase with the current, but cannot exceed $\pm E_b$. The waveform is shown in Fig. 4, in which $E_1 = I_s R_1$ is the amplitude of the voltage that would be present if the limiter were disconnected, and $e_o(\theta)$ is the output voltage. From Fig. 4,

$$E_1 \sin \theta_1 = E_b$$

whence

$$\theta_1 = \sin^{-1}\left[\frac{E_b}{E_1}\right]$$

We shall call θ_1 the "ignition angle" (6), and $\theta_2 = \pi - \theta_1$ the "extinction angle." The angle $\theta_c = \theta_2 - \theta_1$ will be called the "conduction angle," and the corresponding time interval $\left(T_c = \frac{\theta_c}{\omega}\right)$, "conduction period."

The first quarter-cycle of the output voltage is given by

$$e_o(t) = \begin{cases} E_1 \sin \theta, & \text{for } 0 < \theta < \theta_1 \\ E_b = E_1 \sin \theta_1, & \text{for } \theta_1 < \theta < \frac{\pi}{2} \end{cases}$$

This is an odd function containing only odd harmonics and no dc term. Hence, the corresponding Fourier representation is given by

$$e_o(t) = \sum_{k=1}^{\infty} A_K \sin k\theta \qquad k = 1, 3, 5 \ldots$$

where

$$A_K = \frac{4}{\pi} \int_0^{\pi/2} e_o(t) \sin k\theta d\theta$$

It follows that

$$A_K = \frac{4}{\pi}\int_0^{\theta_1} E_1 \sin\theta \sin k\theta d\theta + \frac{4}{\pi}\int_{\theta_1}^{\pi/2} E_1 \sin\theta_1 \sin k\theta d\theta$$

$$= \frac{4E_1}{\pi}\left\{\left[\frac{\sin(k-1)\theta}{2(k-1)} - \frac{\sin(k+1)\theta}{2(k+1)}\right]_0^{\theta_1} + \frac{\sin\theta_1}{k}\left[-\cos k\theta\right]_{\theta_1}^{\pi/2}\right\}$$

$$= \frac{4E_1}{\pi}\left[\frac{\sin(k-1)\theta_1}{2(k-1)} - \frac{\sin(k+1)\theta_1}{2(k+1)} + \frac{\sin\theta_1 \cos k\theta_1}{k}\right]$$

For the fundamental component, k = 1, and we have

$$A_1 = \frac{2E_1}{\pi}\left[\theta_1 + \frac{\sin 2\theta_1}{2}\right] \tag{1}$$

Since $\theta_1 = \sin^{-1}(E_b/E_1)$, we can rewrite Eq. 1 as

$$A_1 = \frac{2E_1}{\pi}\left\{\sin^{-1}\frac{E_b}{E_1} + \frac{E_b}{E_1}\left[1 - \left(\frac{E_b}{E_1}\right)^2\right]^{1/2}\right\} \tag{2}$$

Hence, as far as the fundamental component of the output voltage is concerned, the diode acts as a variable transfer function, the magnitude of which depends on the input amplitude and the bias. It is convenient to define a driving ratio,

$$\eta = \frac{E_1}{E_b} = \frac{I_s R_1}{E_b} \tag{3}$$

which is the ratio of the peak voltage that would appear across the terminals if the limiter were removed, to the bias voltage. Thus, Eq. 2 can be rewritten in terms of η as

$$A_1 = E_1 \cdot \frac{2}{\pi}\left\{\sin^{-1}\frac{1}{\eta} + \frac{1}{\eta}\left[1 - \frac{1}{\eta^2}\right]^{1/2}\right\} \tag{4}$$

The quantity multiplying E_1 in the right-hand member of Eq. 4 will be called the loading factor of the limiter, δ_o. In terms of δ_o, Eq. 4 becomes

$$A_1 = E_1\delta_o = I_s R_1 \delta_o \tag{5}$$

In Fig. 5 the amplitude, A_1, of the fundamental component of the output voltage, is plotted against E_1, for several values of E_6. A glance at Fig. 5 will show that limiting is very good for driving ratios greater than 2. This optimistic result is a consequence of the (also optimistic) assumption that the diodes are ideal. However, this simplified analysis was not a waste of time. We shall use part of the results obtained here in

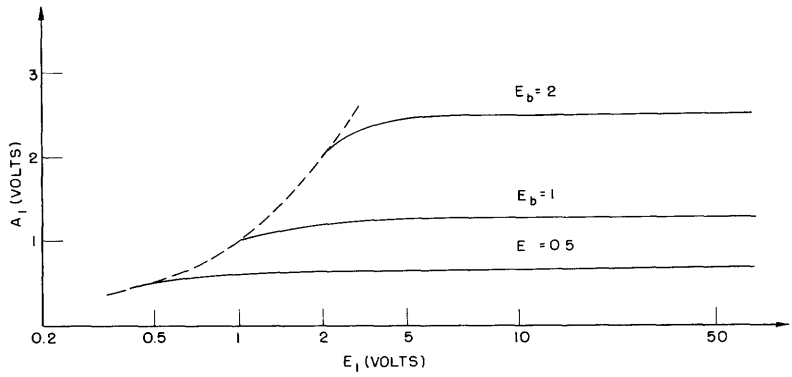

Fig. 5. A_1 versus E_1.

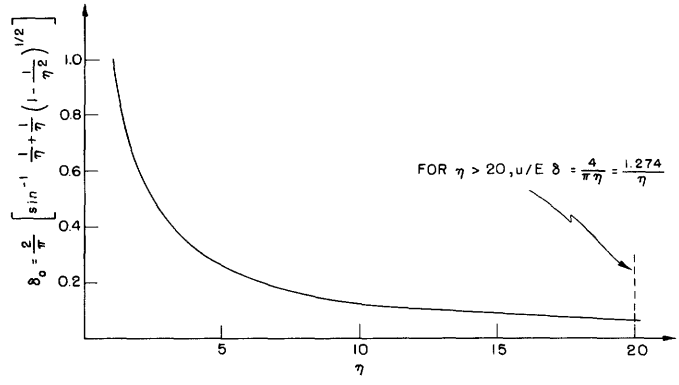

Fig. 6. Loading factor δ_o versus driving ratio η.

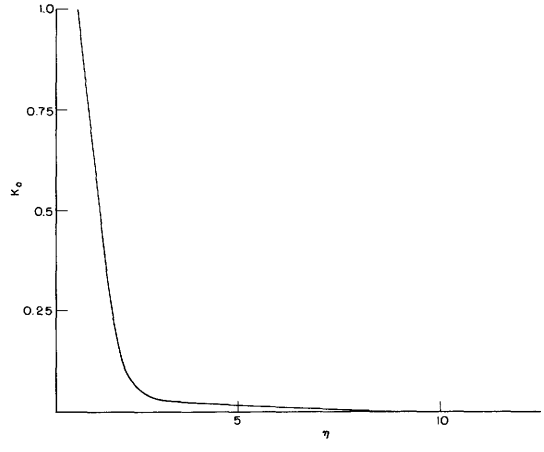

Fig. 7. Limiter coefficient K_o versus η (ideal diodes).

Sections III and IV, where the analysis will be based on nonideal diodes.

Figure 6 shows a plot of the loading factor δ_o as a function of the driving ratio. It is easily seen that, for driving ratios greater than approximately 20, the loading factor becomes $\delta_o \approx 4/\pi\eta$. Hence, for such high values of η, expression 5 becomes

$$A_1 \approx \frac{4E_1}{\pi\eta} = \frac{4E_b}{\pi} \tag{6}$$

This again indicates that, for large driving ratios, limiting is almost perfect, since A_1 is practically independent of E_1.

2.4 LIMITER COEFFICIENT

In a practical situation, it would be desirable to have A_1, the fundamental output voltage, as independent of E_1 as possible. This indicates that a convenient parameter for defining the efficiency of a limiter would be

$$\phi_o = \left[\frac{\partial A_1}{\partial E_1}\right]_{E_b=\text{constant}} \tag{7}$$

However, since the output voltage is reduced by a factor of δ_o with respect to the input voltage, a more realistic parameter is

$$K_o = \frac{\phi_o}{\frac{A_1}{E_1}} = \frac{\phi_o}{\delta_o} \tag{8}$$

which we shall call the "limiter coefficient." Full justification for this choice is given in section 4.3. For the time being, we shall derive an expression for K_o that will be needed later. Expression 7 can be rewritten as

$$\phi_o = \frac{\partial}{\partial E_1}(E_1\delta_o) = \delta_o + E_1\frac{\partial \delta_o}{\partial E_1} \tag{9}$$

It follows that

$$\phi_o = \delta_o + \frac{2}{\pi}\left\{\frac{2E_b}{\left(E_1^2 - E_b^2\right)^{1/2}}\left[\left(\frac{E_b}{E_1}\right)^2 - 1\right]\right\}$$

Substituting for δ_o, we obtain

$$\phi_o = \frac{2}{\pi}\left[\sin^{-1}\frac{E_b}{E_1} - \frac{E_b}{E_1}\left(1 - \left[\frac{E_b}{E_1}\right]^2\right)^{1/2}\right] \tag{10}$$

Thus, in terms of η, we can write

$$K_o = \frac{\phi_o}{\delta_o} = \frac{\left[\sin^{-1}\frac{1}{\eta} - \frac{1}{\eta}\left(1 - \frac{1}{\eta^2}\right)^{1/2}\right]}{\left[\sin^{-1}\frac{1}{\eta} + \frac{1}{\eta}\left(1 - \frac{1}{\eta^2}\right)^{1/2}\right]} \tag{11}$$

It can be easily shown that as $\eta \to \infty$, $K_o \to 0$, which is the agreement with the results of section 2.3. In Fig. 7, K_o has been plotted against η. It is apparent that for $\eta > 12$, $K_o \approx 0$. If the driving ratio is kept above 2, the limiter coefficient is never greater than 0.1. We have already commented on the inadequacy of this particular model, and we shall not waste any more time on it here. We shall come back to a more detailed analysis of the limiter coefficient in Section IV.

III. THE UNBIASED CRYSTAL-DIODE LIMITER

3.1 A USEFUL EQUIVALENT FORWARD DIODE RESISTANCE

The ideal model of a crystal diode has been found to be of limited usefulness. As a model for the study of unbiased limiters it is obviously of no use at all. Since it leads to the prediction of zero output voltage for any value of input voltage, we must adopt a different model.

The volt-ampere characteristic of a crystal diode is nonlinear. The forward resistance decreases as the voltage across the diode increases. For limited regions of operation, a reasonable approximation for this relation is given by

$$i = Av^n \tag{12}$$

where i and v are the forward current and voltage. The constants A and n depend on the particular diode used and the region of operation. Bearing in mind that we are particularly interested in the fundamental component of the output voltage, we can calculate the value of an equivalent constant forward resistance R_D with the property that, if the input current is $i_D = I_D \sin \omega t$, the energy dissipated over one period in the actual diode equals $1/2\ I_D^2 R_D$. Formally,

$$\frac{1}{2} I_D^2 R_D = \frac{1}{2\pi} \int_0^{2\pi} v\, i\, dt$$

$$\frac{1}{2} I_D^2 R_D = \frac{1}{2\pi} \int_0^{2\pi} \left[\frac{I_D}{A} \sin \theta\right]^{1/n} I_D \sin \theta \, d\theta$$

where, according to Eq. 12,

$$v = \left[\frac{i}{A}\right]^{1/n} = \left[\frac{I_D \sin \theta}{A}\right]^{1/n}$$

It follows that

$$R_D = \frac{I_D^{1/n}}{\pi I_D A^{1/n}} \int_0^{2\pi} \left[\sin \theta\right]^{\frac{n+1}{n}} d\theta$$

$$R_D = \frac{4}{\pi A^{1/n} I_D^{(n-1)/n}} \int_0^{\pi/2} [\sin \theta]^m \, d\theta$$

where $m \equiv (n+1)/n$. Upon integration,

$$R_D = \frac{4}{A^{1/n} I_D^{(n-1)/n}} \cdot \frac{\sqrt{\pi}}{2} \cdot \frac{\Gamma\left[\frac{m+1}{2}\right]}{\Gamma\left[\frac{m}{2}+1\right]}$$

Letting

$$\frac{2\Gamma\left[\frac{m+1}{2}\right]}{\sqrt{\pi}A^{1/n}\,\Gamma\left[\frac{m}{2}+1\right]} = K'$$

we have

$$R_D = \frac{K'}{I_D^{(n-1)/n}} \tag{13}$$

Thus, we have found an equivalent resistance whose value depends on the amplitude of the diode current. (See sec. 4.2.) The backward resistance will be assumed to be infinite.

3.2 UNBIASED RESISTIVE MODEL WITH CRYSTAL DIODES

Having agreed upon the equivalent resistance given by expression 13, we proceed to the analysis of a resistive model of the unbiased limiter.

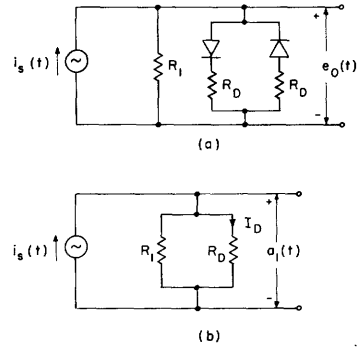

Fig. 8. (a) Resistive model (unbiased nonideal diode).
(b) Equivalent circuit for the fundamental component of the output voltage.

As far as the fundamental component of the output voltage is concerned, the resistive model, shown in Fig. 8a, may be redrawn as in Fig. 8b. It follows that

$$A_1(t) = \left[\frac{R_1 R_d}{R_1 + R_d}\right] I_s \sin t$$

The amplitude of $A_1(t)$ is given by

$$A_1 = I_s R_L \tag{14}$$

where

$$R_L \equiv \frac{R_1 R_D}{R_1 + R_D} \tag{15}$$

or by

$$A_1 = \frac{E_1 R_L}{R_1} \tag{16}$$

Here, E_1 and R_1 are defined as in section 2.3. Following the procedure of Section II, we identify

$$\delta_u = \frac{R_L}{R_1} \tag{17}$$

as the loading factor for the unbiased limiter. Or, if we follow Eq. 15,

$$\delta_u = \frac{R_D}{R_1 + R_D} \tag{18}$$

3.3 PERFORMANCE OF THE UNBIASED LIMITER

3.31 Limiter Coefficient

The limiter coefficient was defined in section 2.4. The equivalent expression for the case of unbiased diodes is

$$K_u = \frac{dA_1/dE_1}{\delta_u} = \frac{\phi_u}{\delta_u} \tag{19}$$

It follows that

$$\phi_u = \delta_u + E_1 \frac{d\delta_u}{dE_1} \tag{20}$$

From the definition of R_D and Fig. 8b, we can write

$$I_D = \frac{A_1}{R_D} = \frac{E_1 \delta_u}{R_D} \tag{21}$$

for the amplitude of the fundamental component of the diode current. Expression 13 becomes

$$R_D = K\left[\frac{R_D}{E_1 \delta_u}\right]^{\frac{n-1}{n}}$$

or

$$R_D = K^n [E_1 \delta_u]^{1-n} \tag{22}$$

Since

$$\delta_u = \frac{R_D}{R_1 + R_D}$$

we have

$$\frac{d\delta_u}{dE_1} = \frac{\delta_u}{R_1 + R_D}\left[\frac{dR_D}{dE_1}\right] \tag{23}$$

and from Eq. 23,

$$\frac{dR_D}{dE_1} = \frac{(1-n)R_D}{\delta_u}\left[\frac{d\delta_u}{dE_1}\right]\frac{(1-n)R_D}{E_1} \tag{24}$$

If we combine the results of Eqs. 23 and 24, we obtain

$$\frac{d\delta_u}{dE_1} = \frac{\delta_u^2(1-n)}{E_1[1 - \delta_u(1-n)]} \tag{25}$$

Finally, the use of Eqs. 19, 20, and 25 yields

$$K_u = \frac{1}{1 + \delta_u(n-1)} \tag{26}$$

The minimum value of K_u is obtained when δ_u approaches one; that is,

$$\lim_{\delta_u \to 1} K_u = 1 \tag{27}$$

Actually, $\delta_u = 1$ requires that $R_1 = 0$, and the limiter is shorted out. It is apparent that large values of n result in better limiting.

Some crystal diodes follow quite closely a square law, that is,

$$i_D = Av_D^2 \tag{28}$$

For n = 2, the diode resistance R_D is given by

$$R_D = \left[\frac{K}{I_D}\right]^{\frac{1}{2}}$$

where $K = \frac{1}{A}$.

The limiter coefficient (Eq. 26) becomes

$$K_u = \frac{1}{1 + \delta_u} \tag{29}$$

The smallest values of K_u occur when $\delta_u \to 1$. In this case,

$$\lim_{\delta_u \to 1} K_u = \frac{1}{2}$$

This implies that 0.5 is an upper limit for the limiter coefficient of an unbiased limiter, unless better diodes (n > 2) are employed. This is poor limiting performance. In Section IV we shall show that biased diodes have comparatively better performance.

IV. THE BIASED CRYSTAL-DIODE LIMITER

4.1 A REVISED APPROACH TO THE RESISTIVE MODEL

The idealized model analyzed in Section II proved to be a very poor approximation of an actual limiter. The analysis of the ideal diode model led us to the conclusion that, except at very low driving ratios (near the limiting threshold), the limiting action is very effective. Measurements performed by Paananen (1) indicate that there is an optimum region of operation, and that the limiter efficiency drops off for both very high and very low driving ratios. We shall try to revise our resistive model by introducing the diode equivalent resistance developed in Section III. A new analysis will be carried out and, with the new results, a set of characteristics will be calculated and plotted.

4.2 ANALYSIS OF THE RESISTIVE MODEL WITH ACTUAL DIODES

The equivalent circuit for this situation is shown in Fig. 9. Here, a square-law diode will be assumed, for which the diode resistance is

$$R_D = \left[\frac{K}{I_D}\right]^{\frac{1}{2}} \tag{30}$$

This is the expression for R_D in Fig. 9. The voltages e_{D_1} and e_{D_2} across the

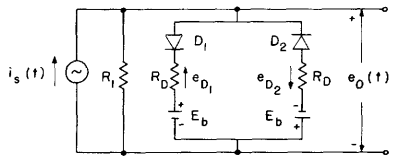

Fig. 9. Resistive model (biased nonideal diode).

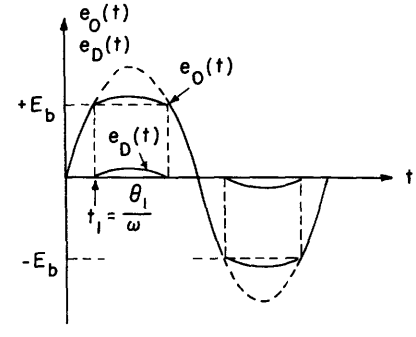

Fig. 10. Output voltage e_o and diode voltage e_D versus time.

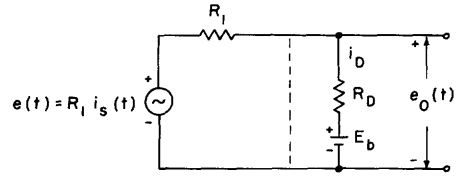

Fig. 11. Equivalent circuit for the conduction period of diode D_1.

equivalent resistances R_D are combined into a single voltage e_D. Figure 10 shows $e_D(t)$.

Diode D_1 starts conducting when $I_s R_1 \sin \theta_1 = E_b$. Whence

$$\theta_1 = \text{arc sin} \frac{E_b}{I_s R_1} = \text{arc sin} \frac{1}{\eta} \tag{31}$$

as in section 2.3. When one of the diodes is conducting, say D_1, the equivalent circuit of Fig. 11 may be used. Hence,

$$i_D = \frac{R_1 i_s(t) - E_b}{R_1 + R_D}$$

or

$$i_D = \frac{R_1 I_s (\sin \theta - \sin \theta_1)}{R_1 + R_D} \tag{32}$$

and

$$e_D = i_D R_D = I_s \frac{R_1 R_D}{R_1 + R_D} (\sin \theta - \sin \theta_1)$$

$$e_o = e_D + E_b = I_s R_L (\sin \theta - \sin \theta_1) + E_b \tag{33}$$

where $R_L = (R_1 R_D)/(R_1 + R_D)$.

The first quarter-cycle of the output voltage is given by

$$e_o(t) = \begin{cases} E_1 \sin \theta, & \text{for } 0 < \theta < \theta_1 \\ E_b + I_s R_L (\sin \theta - \sin \theta_1), & \text{for } \theta_1 < \theta < \pi/2 \end{cases}$$

Again, the function is odd and symmetrical about $\pi/2$, and so

$$e_o = \sum_{k=1}^{\infty} A_K \sin k\theta, \qquad \text{with } k = 1, 3, 5 \ldots$$

where

$$A_K = \frac{4}{\pi} \int_0^{\pi/2} e_o(t) \sin k\theta \, d\theta$$

It follows that

$$A_K = \frac{4}{\pi} \left[\int_0^{\theta_1} E_1 \sin \theta \sin k\theta \, d\theta + \int_{\theta_1}^{\pi/2} E_1 \sin \theta_1 \sin k\theta \, d\theta \right.$$

$$\left. + \int_{\theta_1}^{\pi/2} I_s R_L (\sin \theta - \sin \theta_1) \sin k\theta \, d\theta \right]$$

The first two terms in the right-hand member have already been evaluated (Eq. 1). The last term yields

$$B_K = \frac{4I_s R_L}{\pi}\left[\int_{\theta_1}^{\pi/2} \sin\theta \sin k\theta \, d\theta - \int_0^{\pi/2} \sin\theta_1 \sin k\theta \, d\theta\right]$$

$$B_K = \frac{4I_s R_L}{\pi}\left\{\left[\frac{\sin(k-1)\theta}{2(k-1)} - \frac{\sin(k+1)\theta}{2(k+1)}\right]_{\theta_1}^{\pi/2} - \frac{\sin\theta_1}{k}\left[\cos k\theta\right]_{\theta_1}^{\pi/2}\right\}$$

For the fundamental component, k = 1, and

$$B_1 = \frac{4I_s R_L}{\pi}\left[\frac{\pi}{4} - \frac{\theta_1}{2} + \frac{\sin 2\theta_1}{4} - \sin\theta_1 \cos\theta_1\right]$$

Using Eq. 1, we find, for the total fundamental component,

$$A_1 = \frac{2I_s R_1}{\pi}\left[\theta_1 + \frac{\sin 2\theta_1}{2}\right] + \frac{4I_s R_L}{\pi}\left[\frac{\pi}{4} - \frac{\theta_1}{2} - \frac{\sin 2\theta_1}{4}\right]$$

$$A_1 = \frac{2I_s}{\pi}\left\{R_1\left[\theta_1 + \frac{\sin 2\theta_1}{2}\right] - R_L\left[\theta_1 + \frac{\sin 2\theta_1}{2}\right]\right\} + I_s R_L$$

or

$$A_1 = \frac{2I_s}{\pi}\left\{\left[R_1 - R_L\right]\left[\theta_1 + \frac{\sin 2\theta_1}{2}\right] + \frac{\pi R_L}{2}\right\} \tag{34}$$

However, since

$$\frac{2}{\pi}\left[\theta_1 + \frac{\sin 2\theta_1}{2}\right] = \delta_o$$

expression 34 becomes

$$A_1 = I_s\left[(R_1 - R_L)\,\delta_o + R_L\right] \tag{35}$$

We shall now find the fundamental component of the diode current. Again, the current through the diodes is actually composed of two pulsed currents, flowing in alternate half-cycles in each diode. However, we are going to assume that the diodes have equal resistances, and hence we can simplify matters by recognizing one total diode current $i_D(t)$. The waveform is the same as that for $e_D(t)$, which will be shown in Fig. 13.

Equation 32 is valid for $\theta_1 < \theta < \theta_2$. Since $R_L \equiv (R_1 R_D)/(R_1 + R_D)$, we have

$$I_D(t) = \begin{cases} 0, & \text{for } 0 < \theta < \theta_1 \\ \dfrac{I_s R_L}{R_D}(\sin\theta - \sin\theta_1), & \text{for } \theta_1 < \theta < \pi/2 \end{cases}$$

and the Fourier analysis follows the same lines. For the fundamental component, we find

$$I_D = \frac{4I_s R_L}{\pi R_D}\left[\frac{\pi}{4} - \frac{\theta_1}{2} - \frac{\sin 2\theta_1}{4}\right]$$

or

$$I_D = \frac{R_L}{R_D}\left[I_s - \frac{2I_s}{\pi}\left[\theta_1 + \frac{\sin 2\theta_1}{2}\right]\right]$$

or, in terms of δ_o,

$$I_D = \frac{I_s R_L}{R_D}(1 - \delta_o) \tag{36}$$

We recall that for the ideal diode, the fundamental component of $e_o(t)$ was found to be $A_1 = I_s R_1 \delta_o$; and since for $\eta > 20$, $\delta_o \approx 4/\pi\eta$, we have for large driving ratios,

$$A_1 \approx \frac{E_1}{E_b} \times E_b \times \frac{4}{\pi\eta} = \frac{4E_b}{\pi}$$

Therefore we find that limiting is very good for large driving ratios. Expression 35 gives, for a real diode,

$$A_1 = I_s(R_1 - R_L)\,\delta_o + I_s R_L$$

Here, the first term in the right-hand member becomes roughly constant for large driving ratios. However, the second term shows that, for large driving ratios, the limiter will behave essentially like a resistance R_L, and limiting will be poor. So far, our approximation is qualitatively correct. In a later section, we shall compare theoretical and experimental results and show that, if the values of R_D are chosen carefully, the agreement is very good, if not in absolute values, at least in the shape and slopes of the characteristic.

4.3 LIMITER COEFFICIENT WITH REAL DIODES

In Section II we pointed out that the performance of the limiter could be adequately described by a limiter coefficient, K_o, given by Eq. 8. At that point, we gave no justification for this particular choice. We avoided further discussion of K_o for ideal diodes, since we felt that there was no point in wasting time and effort with a model that would fall short of our expectations. However, the situation here is different, and we expect the limiter coefficient to have a minimum for intermediate driving ratios. The region around this minimum is evidently the optimum region for the operation of the limiter. Consequently, a detailed investigation of the behavior of K_o should be made. We retrace the steps leading to the definition of K_o. We are interested in establishing a relation between the degree of amplitude modulation of the input signal, $m = (E_{max} - E_o)/E_o$, where E_o is the unmodulated amplitude, and the degree of modulation of the output signal. Here we run into difficulties, because the simple concept of degree

of modulation cannot be applied easily to the output voltage.

Let us rewrite expression 35 as follows:

$$A_1 = E_1 \left\{ \left[1 - \frac{R_L}{R_1} \right] \delta_o + \frac{R_L}{R_1} \right\} \tag{37}$$

and define a new loading factor,

$$\delta_L = \delta_o \left[1 - \frac{R_L}{R_1} \right] + \frac{R_L}{R_1} \tag{38}$$

with the result that

$$A_1 = E_1 \, \delta_L \tag{39}$$

It must not be forgotten that δ_L itself is a function of the driving ratio, and hence a function of E_1. To emphasize this point, we rewrite Eq. 39 as

$$A_1 = E_1 \, \delta_L(E_1) \tag{40}$$

If the input voltage is given by

$$e_1(t) = E \, (1+m \sin \omega_m t) \sin \omega_o t$$

the variable input amplitude can be expressed as

$$E_1(t) = E \, (1+m \sin \omega_m t) \tag{41}$$

It is easy to show that the degree of modulation of the input voltage is

$$\frac{E_{max} - E}{E} = \frac{E \, (1+m) - E}{E} = m$$

However, for the output voltage,

$$A_1(t) = E_1(t) \, \delta_L(E_1)$$

$$= E \, (1+m \sin \omega_m t) \, \delta_L(E_1)$$

The maximum value of $A_1(t)$ is

$$A_{max} = E \, (1+m) \, \delta_{L1} = E_{max} \, \delta_{L1}$$

where $\delta_{L1} = \delta_L(E_{max})$. On the other hand, the unmodulated value of $A_1(t)$ is $A_1 = E \, \delta_{L2}$, where $\delta_{L2} = \delta_L(E)$, and thus the degree of modulation becomes

$$\frac{A_{max} - A_1}{A_1} = \frac{E \, (1+m) \, \delta_{L1} - E \, \delta_{L2}}{E \, \delta_{L2}}$$

If we call m_L the degree of modulation at the output of the limiter, we have

$$m_L = m \frac{\delta_{L1}}{\delta_{L2}} + \frac{\delta_{L1} - \delta_{L2}}{\delta_{L2}} \tag{42}$$

It is apparent that δ_L is a complicated function of the driving ratio, and hence there is no simple way of rewriting expression 42. Besides, it must be remembered that, even if the input signal is symmetrically modulated, the output signal will, in general, be symmetrically modulated, because of the nonlinearity of the transfer function. Thus, we would have to deal with two different degrees of modulation: positive peak modulation (m^+) and negative peak modulation (m^-). To simplify matters to a certain extent, we might choose one of them (m^+ or m^-) as the standard output degree of modulation. Then, for given values of E_1 and m, the corresponding values of δ_L might be taken from a graph and Eq. 42 would yield m_L. If, however, we use Eq. 42 to define the limiter coefficient, we can write

$$m_L = m \left[\frac{\delta_{L1}}{\delta_{L2}} + \frac{1}{m} \frac{\delta_{L1} - \delta_{L2}}{\delta_{L2}} \right]$$

In this expression, the quantity in brackets would be the limiter coefficient, which clearly depends on the input degree of modulation m.

The preceding difficulties have led us to define the limiter coefficient as

$$K_L = \frac{\left[\frac{\partial A_1}{\partial E_1}\right]_{E_b=\text{constant}}}{\frac{A_1}{E_1}} \tag{43}$$

For a given E_b, we can write

$$\frac{dA_1}{A_1} = K_L \frac{dE_1}{E_1}$$

For small increments, this reduces to

$$\frac{\Delta A_1}{A_1} \approx K_L \frac{\Delta E_1}{E_1} = K_L m$$

For large degrees of modulation, K_L loses the simple interpretation given above. However, if the values of K_L are plotted against input voltage, the result should show the most efficient range of operation for each value of E_b. This range would obviously be characterized by low values of K_L.

Now, let

$$\phi_1 = \left[\frac{\partial A_1}{\partial E_1}\right]_{E_b=\text{constant}}$$

From Eq. 37, we have

$$A_1 = E_1 \delta_o - E_1 \delta_o \frac{R_L}{R_1} + E_1 \frac{R_L}{R_1}$$

It follows that

$$\phi_1 = \delta_o \left[1 - \frac{R_L}{R_1}\right] + \frac{R_L}{R_1} + \left\{E_1 \left[1 - \frac{R_L}{R_1}\right]\right\} \frac{\partial \delta_o}{\partial E_1} + \left[\frac{E_1}{R_1}(1 - \delta_o)\right] \frac{\partial R_L}{\partial E_1} \tag{44}$$

With the use of Eq. 9 we obtain

$$\frac{\partial \delta_o}{\partial E_1} = \frac{\phi_o - \delta_o}{E_1} \tag{45}$$

From Eqs. 44 and 45 we have

$$\phi_1 = \delta_o \left[1 - \frac{R_L}{R_1}\right] + \frac{R_L}{R_1} + [\phi_o - \delta_o] \left[1 - \frac{R_L}{R_1}\right] + \frac{E_1}{R_1}(1 - \delta_o) \frac{\partial R_L}{\partial E_1}$$

or

$$\phi_1 = \phi_o \left[1 - \frac{R_L}{R_1}\right] + \frac{R_L}{R_1} + \frac{E_1}{R_1}(1 - \delta_o) \frac{\partial R_L}{\partial E_1} \tag{46}$$

Since $R_L = (R_1 R_D)/(R_1 + R_D)$, we have

$$\frac{\partial R_L}{\partial E_1} = \left[\frac{R_L}{R_D}\right]^2 \frac{\partial R_D}{\partial E_1} \tag{47}$$

Again, Eqs. 31 and 38 yield

$$R_D^2 = \frac{K}{I_D}$$

$$\frac{R_D}{R_L} = \frac{I_s}{I_D}(1 - \delta_o)$$

whence

$$\frac{R_1 + R_D}{R_D^2} = \frac{E_1(1 - \delta_o)}{K}$$

$$\frac{R_D^2 - 2R_D(R_1 + R_D)}{R_D^4} \frac{\partial R_D}{\partial E_1} = \frac{1 - \delta_o}{K} - \frac{E_1 \frac{\partial \delta_o}{\partial E_1}}{K}$$

$$\left[\frac{-R_D - 2R_1}{R_D^3}\right] \frac{\partial R_D}{\partial E_1} = \frac{1 - \delta_o - \phi_o + \delta_o}{K} = \frac{1 - \phi_o}{K}$$

$$\frac{\partial R_D}{\partial E_1} = \frac{R_D^3}{R_D + 2R_1} \frac{(\phi_o - 1)}{K} \tag{48}$$

Substituting Eq. 48 in Eq. 47, we find that

$$\frac{\partial R_L}{\partial E_1} = \frac{R_L^2 R_D}{R_D + 2R_1} \frac{(\phi_o - 1)}{K} \tag{49}$$

Using Eqs. 46 and 49, we obtain

$$\phi_1 = \phi_o \left[1 - \frac{R_L}{R_1} \right] + \frac{R_L}{R_1} + \frac{E_1}{R_1} \frac{(1 - \delta_o)(\phi_o - 1)}{K} \frac{R_L^2 R_D}{R_D + 2R_1}$$

Finally,

$$K_L = \frac{\frac{\phi_1}{A_1}}{\frac{E_1}{}} = \frac{\phi_1}{\left[1 - \frac{R_L}{R_1} \right] \delta_o + \frac{R_L}{R_1}}$$

or

$$K_L = \frac{\phi_o(R_1 - R_L) + R_L + \frac{E_1}{K} \frac{R_L^2 R_D}{R_D + 2R_1} (1 - \delta_o)(\phi_o - 1)}{\delta_o(R_1 - R_L) + R_L} \tag{50}$$

Since

$$R_L^2 = \frac{R_D^2 R_1^2}{(R_1 + R_D)^2}$$

and

$$R_D^2 = \frac{K(R_1 + R_D)}{E_1(1 - \delta_o)}$$

Eq. 50 becomes

$$K_L = \frac{\phi_o(R_1 - R_L) + R_L + (\phi_o - 1) \frac{R_L R_1}{R_D + 2R_1}}{\delta_o(R_1 - R_L) + R_L} \tag{51}$$

where ϕ_o, defined in expression 7, is given by Eq. 10. We have now obtained the general expression. It can be simplified for high driving currents.

Consider

$$\frac{R_L R_1}{R_D + 2R_1} = \frac{R_L}{\frac{R_D}{R_1} + 2}$$

Even for moderate currents $R_D/R_1 \ll 2$, and

$$\frac{R_L}{\frac{R_D}{R_1} + 2} \approx \frac{R_L}{2}$$

(In Section V, R_D is plotted against I_s. See Fig. 12.) Hence, Eq. 51 can be rewritten as

$$K_L = \frac{\phi_o(R_1 - R_{L/2}) + R_{L/2}}{\delta_o(R_1 - R_L) + R_L} \tag{52}$$

If we substitute for R_L its expression in terms of R_D and R_1, Eq. 52 can be simplified to

$$K_L = \frac{\phi_o(2R_1 + R_D) + R_D}{2(\delta_o R_1 + R_D)} \tag{53}$$

The asymptotic behavior of K_L for both large and small driving ratios is not difficult to investigate. It is apparent that when η decreases and approaches 1, K_L will approach 1, because if the voltage developed across the limiter becomes smaller than the bias, all of the variations in the input amplitude are reproduced without change. On the other hand, for very large driving ratios, both ϕ_o and δ_o approach zero very quickly. Hence, Eq. 53 becomes

$$K_L \approx \frac{R_D}{2R_D} = \frac{1}{2} \tag{54}$$

It will be shown (see section 5.2) that K_L does not decrease steadily from 1 to 0.5, but goes through an intermediate region where its values are considerably lower than 0.5. Hence, 0.5 is actually the worst value of K_L, except for the region of low driving ratios. It is interesting at this point to recall from Eq. 29 that the best value for the limiter coefficient of unbiased square-law diodes was 0.5. The improvement brought about by the use of bias is apparent. But it is obvious that the limiter must be operated in the appropriate region, otherwise the advantage is lost.

Admittedly, the large amount of algebraic manipulation through which we have waded may have obscured the significance of the results. In Section V all of the relevant expressions will be brought together, and plots will be shown for particular practical values of the variable.

V. THEORETICAL AND EXPERIMENTAL PERFORMANCE OF THE RESISTIVE MODEL

5.1 ESSENTIAL RESULTS OF THE THEORETICAL ANALYSIS

Assuming that we have the design of a limiter in mind, the essential information we would like to secure would all be contained in a set of characteristics for several representative values of bias. The slope of the characteristics at any point will give a rough indication of the value of K_L at that point. Specifically, if the slope is zero, K_L is zero (perfect limiting). But it would also be desirable to have K_L plotted directly against driving current and bias. This eliminates the need for guessing the limiting properties by inspection of the characteristics and provides a convenient way of predicting the performance of the limiter for a given set of operating conditions.

The first step toward a better understanding of the conclusions reached thus far is to summarize the relevant results of Sections II-IV.

If we assume a square-law behavior for the crystal diodes, R_D (equivalent resistance of the diode) and I_D (peak diode current) are given by a pair of equations:

$$R_D^2 = \frac{K}{I_D} \tag{55a}$$

$$I_D = \frac{I_s R_1}{R_1 + R_D}(1 - \delta_o) \tag{55b}$$

where R_1 is the parallel resistance across the limiter, I_s is the peak value of the input current, and δ_o is the loading factor, given by Eq. 2 and plotted in Fig. 6.

The fundamental component of the output voltage will have an amplitude given by

$$A_1 = I_s[(R_1 - R_L)\,\delta_o + R_L] \tag{56}$$

where I_s and R_1 are as defined by Eqs. 55a and 55b, and $R_L = (R_D R_1)/(R_D + R_1)$. The limiter coefficient, K_L, is given by Eq. 51.

These are the essential results. They do not look particularly helpful in the present form. Therefore let us investigate their behavior for appropriate values of I_s, R_1, R_D, and E_b. The choice of values for these variables is motivated by the results of measurements that had previously been made on a resistive model of the diode limiter. Paananen (1) plotted the characteristics of a diode limiter at 60 cps, for current drives from 0.1 to 60 ma (rms) and several values of E_b, ranging from 0.25 to 10 volts.

These are the ranges that we shall use in our calculations. In section 5.3, a correlation of theoretical and experimental results will be carried out.

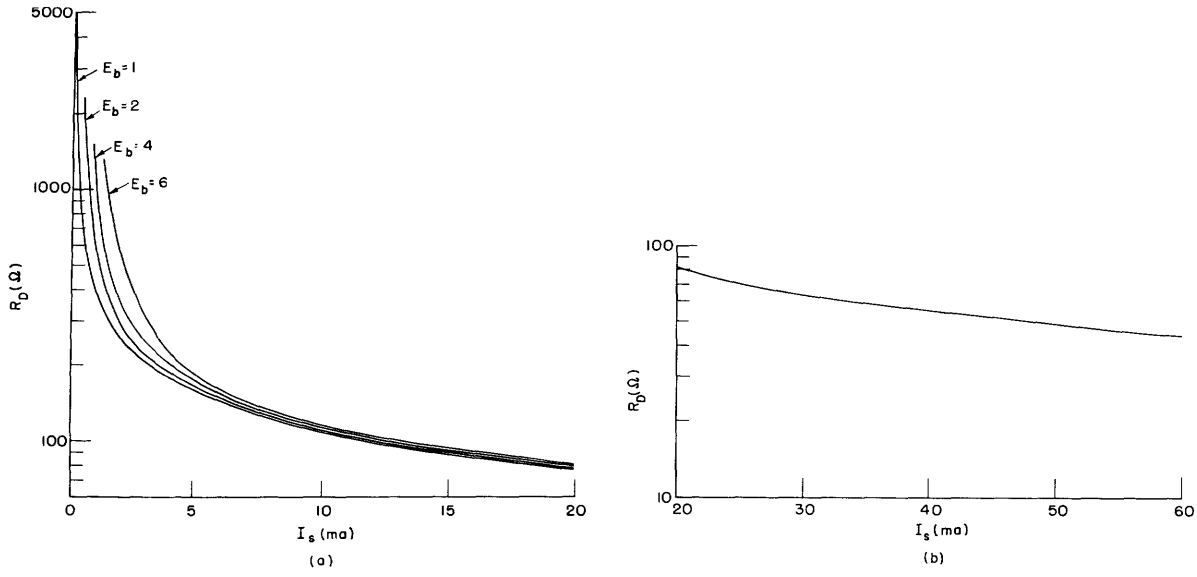

Fig. 12. Equivalent diode resistance R_D versus driving current I_S (peak).

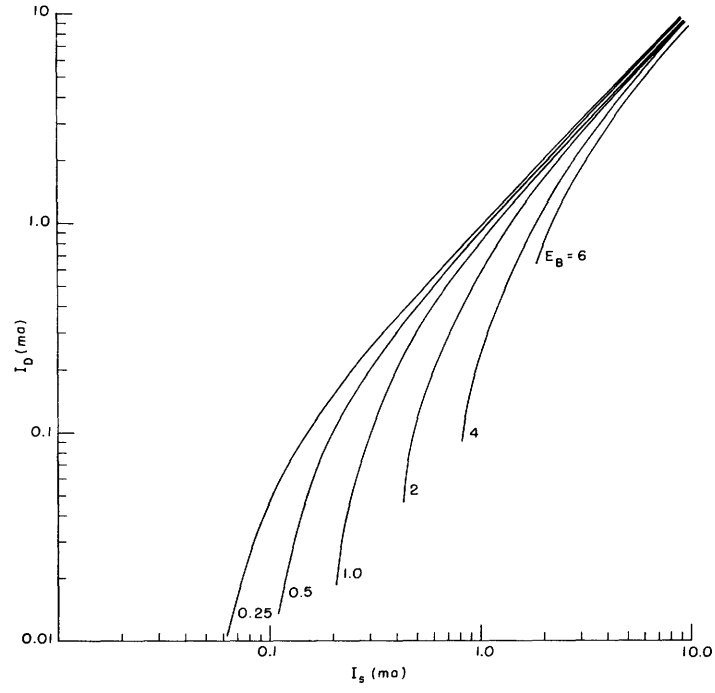

Fig. 13. Diode current I_D (fundamental) versus driving current I_S (peak).

5.2 THEORETICAL CHARACTERISTICS OF THE RESISTIVE MODEL

5.21 Calculations for R_1 = 6000 ohms

Paananen's measurements assumed an equivalent tank-circuit resistance of 6000 ohms, for which his plots show rms values of $A_1(t)$ (fundamental component of the output voltage) plotted against $i_D(t)$, the diode current. We felt that a plot of $a_1(t)$ versus $i_s(t)$ (the driving current) would be more useful, since the diode current is not an independent variable in our problem. The type of diode employed for the measurements was not mentioned by Granlund (1). The unbiased characteristics shown, however, match closely those of a 1N34 crystal diode. Since we are not really interested in any particular diode, as long as the square-law approximation is valid, we have decided to use a 1N34 diode for our calculations.

Inspection of curves from 1N34 data in the region of interest shows that for this diode (6) the constant K in Eq. 55a may be taken as K = 120.

The solution of the auxiliary equations (Eqs. 55a and 55b) is shown in Fig. 12a and b and in Fig. 13. They have one feature in common: for large values of I_s, both R_D and I_d are practically independent of E_b. Physically, this indicates that the harder we drive the limiter, the closer it will approach the unbiased model. For large I_s, we notice that $I_d \approx I_s$, which shows that the diodes are closed practically all the time, regardless of bias. These curves are not important by themselves, but they have been used for later calculations, and so they are included for later reference.

The limiter characteristics are shown in Fig. 14. The straight line, common to all of the curves, has the slope associated with R_1 = 6000 ohms. The limiter operates along this line until the voltage reaches E_b. Beyond this point, the operation shifts over

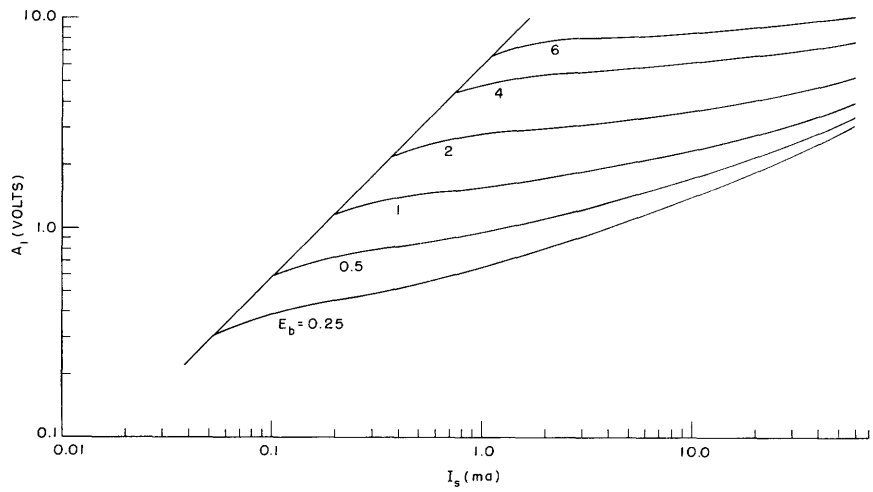

Fig. 14. Resistive limiter characteristics: fundamental component of the output voltage A_1 (peak) versus driving current I_s (peak). R_1 = 6000 ohms.

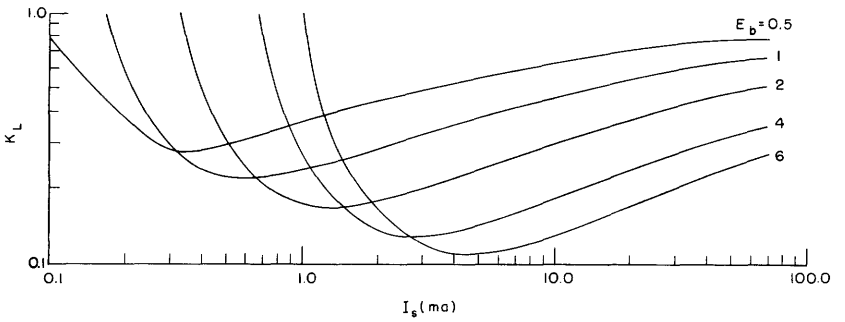

Fig. 15. Limiter coefficient K_l versus driving current. R_l = 6000 ohms.

to the corresponding bias curve. The improvement of linearity and slope with increasing values of E_b is striking. However, in this case, higher driving ratios are required. Figure 14 also shows that, for high percentages of modulation, the voltage will drop more frequently below the bias. This condition is most undesirable, because there is no limiting at all when the limiter is not driven above E_b. The characteristics may be used for computing the reduction in amplitude modulation by entering the axis of the abscissas with the maximum and minimum amplitudes of the input current and reading off the corresponding limits of the output voltage.

A more convenient and meaningful plot is the one for K_L, shown in Fig. 15. The outstanding information conveyed by Fig. 15 is that K_L is large for both very high and very low driving currents, and is minimum for intermediate drives. It should be noted that the region around which K_L is minimum depends on the bias; the values of I_s increase as the bias increases. Also, the minimum values for large bias are much smaller than those for small bias, which, again, shows the superior performance of high-biased diodes.

The approximate reduction in amplitude modulation may be found (except for modulation factors larger than 0.9) by taking the average K_L for the given input current amplitude. The shape of the curves shows that this average will necessarily be higher for larger excursions. This indicates that the limiter effectiveness decreases as the degree of modulation increases. The appropriate operation of the limiter for high degrees of modulation seems to be at low bias and hard drive. This can be visualized roughly by the following considerations. For very large driving currents, K_L approaches 0.5, as was shown in section 4.3. (The curves in Fig. 15 were not extended far enough to show this limiting value, but the general trend of the curves is apparent.) On the other hand, below the limiting threshold K_L equals 1. It is likely that the average value of K_L will be smaller if K_L never reaches 1. At low bias, although K_L is comparatively larger for large drives, it remains much longer below 1 in the low-current region. If the degree of modulation is expected to be low or moderate, the best region of operation may be chosen. Aside from other design considerations, high bias and the driving that minimizes K_L should be used. For instance, a 50 per cent modulated current of 6 ma

average (I_{max} = 9 ma, I_{min} = 3 ma) for a bias of 6 volts will have a reduction in modulation of approximately 90 per cent per stage, so that after two stages of limiting the modulation should drop to approximately 0.5 per cent.

In conclusion, the results of this preliminary analysis seem to indicate that, if several stages of limiting are used, the maximum effectiveness will be achieved (with a minimum number of stages) by using hard-driven low-biased stages as prelimiters, followed by high-biased stages with optimum drive.

5.22 Calculations for R_1 = 10,000 ohms

In the expression for the limiter coefficient (Eq. 9), it is apparent that a reduction in K_L will be achieved if the ratio A_1/E_1 is increased for a given slope $\partial A_1/\partial E_1$. It is not easy to tell at a glance how expressions 51, 55, and 56 should be modified in order for this condition to obtain. However, we did not feel that it would be worth while to compute partial derivatives of all the unknowns (for example, A_1 and K_L) with respect to each of the independent variables (E_b, I_s, R_1, etc.) in order to determine the maxima of A_1/E_1 and K_L. If the resistive model proves to be of any use at all as an

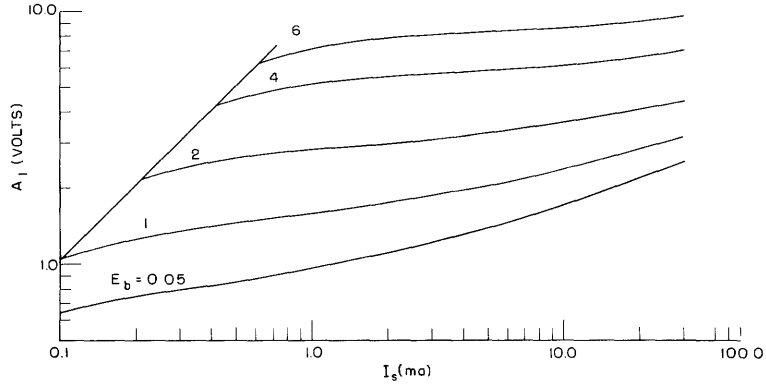

Fig. 16. Limiter characteristics. R_1 = 10,000 ohms.

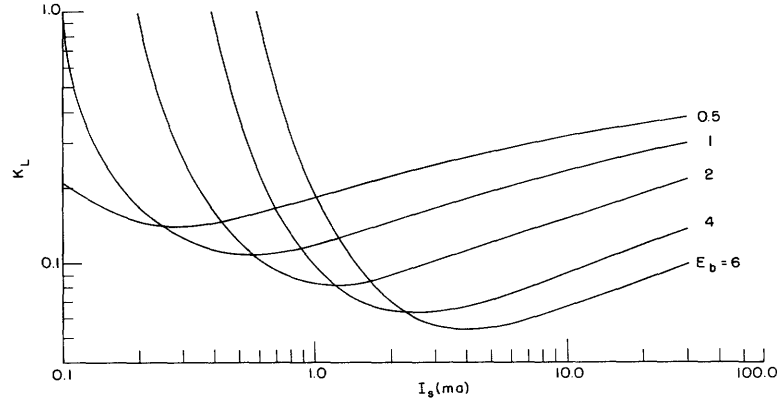

Fig. 17. Limiter coefficient K_L. R_1 = 10,000 ohms.

approximation, it certainly would be desirable to carry out this kind of investigation. Since our plots covered fairly wide ranges of input current and bias, we decided that the next thing to do was to try some other value of R_1.

Figure 16 shows a set of limiter characteristics for R_1 = 10,000 ohms. Except that all curves in the low-current region are shifted upward, these curves look very much like those of Fig. 14.

Although there is no apparent improvement, Fig. 17, in which K_L is plotted for this case, shows a substantial reduction in K_L for <u>all</u> ranges of I_s and E_b. This is a point in favor of our adoption of K_L as a representative parameter of the limiter efficiency. If we take the numerical example used in section 5.21 (6 ma average, with 50 per cent modulation), the reduction per stage is found to be almost 95 per cent. After two stages of limiting, the modulation should be reduced to approximately 0.16 per cent. It might be argued that the same information could be taken from the characteristics, but in a set of K_L curves the limiting properties of any region of operation can be found very easily by inspection.

The reason why we insist so much on the usefulness of the limiter coefficient, as defined here, is that we believe that the choice of K_L is not attached to the use of a resistive model. Even if the resistive model proves to be a bad approximation, the limiter coefficient will retain its usefulness, and may be appropriately introduced in a more refined treatment of the problem.

5.3 CORRELATION OF EXPERIMENTAL AND THEORETICAL RESULTS

We are now in a position to compare the essential results of our theory with the experimental data. In Fig. 18 theoretical and experimental curves are plotted, for

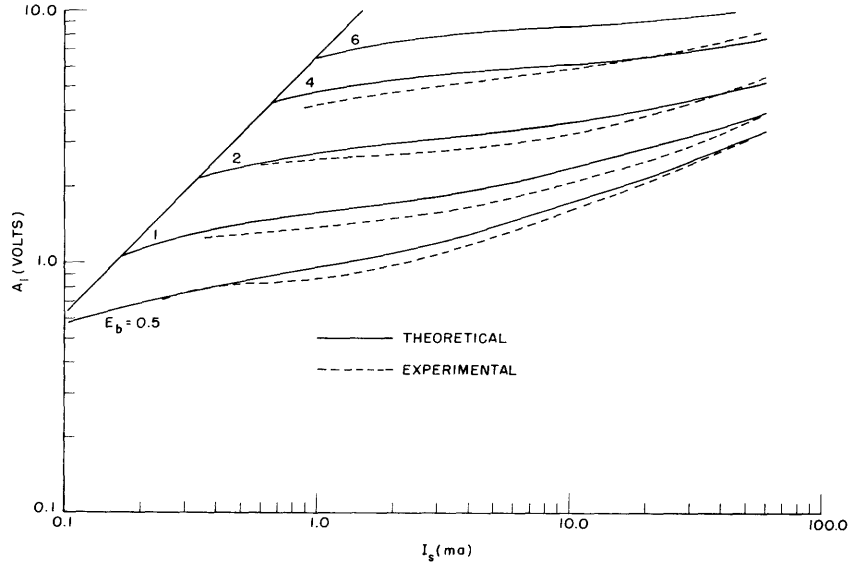

Fig. 18. Limiter characteristics (resistive model). R_1 = 6000 ohms.

E_b = 0.5, 1, 2, and 4. The agreement is better than was expected. The error is below 10 per cent almost everywhere, and it never exceeds 15 per cent. More important than absolute values is the shape of the characteristics, since limiting, as we have shown, is a function of the slope at any point. It is apparent that a large portion of the curves could be brought into coincidence by translation. Our theory seems therefore to be valid for resistive limiters. It should be pointed out, however, that we have not proved the validity of the resistive model. The experimental curves were plotted by Paananen under the assumption that the resistive model was a good approximation for an actual FM limiter. All we have proved after going through all this algebra is that the power law, and in particular the square law, is a close approximation to the actual behavior of a crystal diode. However, we do feel that the methods employed and the insight gained by this simplified theory will be helpful when a more rigorous treatment is attempted.

VI. THE TUNED IDEAL DIODE LIMITER

6.1 A NEW ATTEMPT AT THE SOLUTION OF THE LIMITER PROBLEM

The analysis of the resistive model outlined the answers to a few interesting questions. The validity of the square-law diode is one of them, and the usefulness of the limiter coefficient is another. A point that may have passed unnoticed was the superposition of solutions made in Section IV.

We used the breakpoints, as calculated in Section II, and introduced an equivalent resistance to account for dissipation in the diodes. The conduction periods were tacitly assumed to remain unchanged in the transition from ideal to nonideal diodes. The agreement obtained between theoretical and experimental results shows that the assumption was not unrealistic.

We might hope, therefore, that ideal diodes are sufficiently good models if we are interested in the conduction periods only.

This points a new way out of our problem. We bring into the picture a tuned circuit, which complicates the problem but is essential if we want to know a little more about limiters, but at the same time go back to ideal diodes. This is a more tractable problem than the general one. It may not give us the final answers, but we hope to get good approximations for the conduction periods. Later on, we may try to introduce nonideal diodes, by the methods used in Section IV.

6.2 BREAKPOINT ANALYSIS OF THE TUNED LIMITER

Before we actually carry out the details of the analysis we have in mind, a few remarks are necessary in order to justify some simplifying assumptions that will be made later.

The circuit of Fig. 19a is pertinent to the present situation. In an actual limiter circuit we must take into consideration the resistance of the coil windings in the tuned circuit. This is generally done by including an RL series branch, which, together with the associated capacitance, forms what is sometimes called a parallel-coil-condenser circuit (see Fig. 19b).

It is usual procedure to replace this circuit by an equivalent parallel RLC circuit (7). The substitution is valid for moderate and high Q's. This will always be the case for FM limiters. If we assume a center frequency of 10 mc and an intermediate frequency bandwidth of 200 kc (usual values for FM design), the likely minimum Q can easily be computed.

Baghdady (8) showed that the required bandwidth for interference rejection (for all interference ratios that are less than 0.98) need not exceed three IF bandwidths. We would then have to deal with minimum Q's of approximately

$$Q_{min} = \frac{10^7}{6 \times 10^5} \approx 16$$

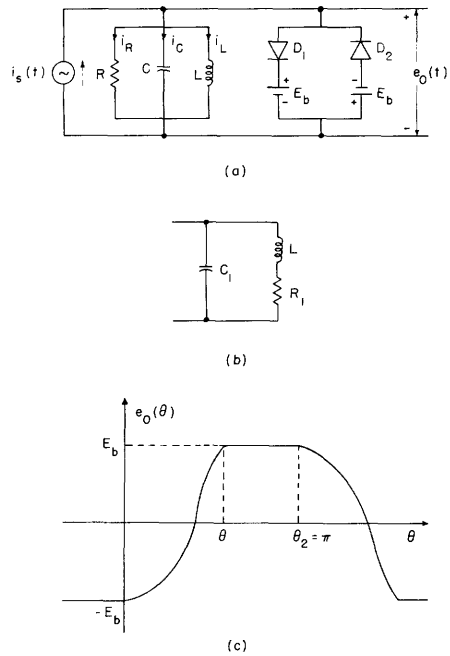

Fig. 19. (a) Biased limiter shunted by tuned circuit (ideal diodes). $[i_s(t) = I_s \cos(\omega t + \phi)]$.
(b) Equivalent tuned circuit that is valid for high Q's.
(c) Output voltage of the tuned limiter.

This is high enough to justify the circuit equivalence and to warrant the use of the usual high-Q approximations.

In Fig. 19a, R is the parallel combination of the equivalent shunt resistance of the coil

$$\left[\text{Req} = \left[\frac{(\omega_o L)^2}{R_1} \right] \right]$$

and the external resistances connected across the circuit (together with the equivalent resistance of the vacuum tube preceding the stage). The condenser C accounts for all capacitances, lumped, stray or wiring that appear across the coil.

The analysis of the circuit of Fig. 19a may seem conceptually easy, but actually great care must be taken to avoid unduly complicated expressions that would entirely obscure the meaning of the results, and probably introduce computational errors.

The best approach was found to be the one based on Fig. 19c. The driving-current phase angle ϕ is left undetermined, while the time origin is taken as the breakpoint of diode D_2, as shown.

This procedure was suggested by an analysis carried out by Madsen (9) in a study of amplitude-to-phase conversion in clippers.

The initial conditions are dictated by physical considerations. Since the diodes are

ideal, during the conduction period the current source is shorted out, and the voltage is clamped at $\pm E_b$. Hence, the current in a resistance is $i_R = \pm E_b/R$, the current in the condenser is zero $[i_c = C\, dv/dt = 0]$, and the current in the coil is a ramp function, given by

$$i = i_o + \frac{E_b}{L}\,\Delta t$$

where $\Delta t = (\theta_2 - \theta_1)/\omega$.

At $\theta = 0$, diode D_2 opens. We are left with a parallel RLC circuit with initial voltage and current, facing a current source of phase ϕ, which is to be determined. The breakpoint of the diode demands that $v_D = i_D = 0$. It follows that

$$e_c(0) = e_o(0) = -E_b \tag{57a}$$

$$i_L(0) = i_S(0) - i_R(0) = I_s \cos\phi + \frac{E_b}{R} \tag{57b}$$

At $\theta = \theta_1$, we can write $e_o(\theta_1) = E_b$. Since we have fixed the breakpoint of D_2 at $\theta = 0$, the symmetry of the circuit requires that $\theta_2 = \pi$.

At $\theta = \theta_2 = \pi$, we have

$$e_o(\pi) = E_b$$

$$i_L(\pi) = I_s \cos(\pi+\phi) - \frac{E_b}{R} = -I_s \cos\phi - \frac{E_b}{R} \tag{58}$$

We can find the current in the coil at $\theta = \theta_1$ in terms of $i_L(\pi)$ if we recall that from $\theta = \theta_1$ to $\theta = \pi$ the increment of i_L is given by a ramp. Thus

$$i_L(\pi) = i_L(\theta_1) + \frac{E_b}{L}\,\frac{(\pi - \theta_1)}{\omega}$$

Hence, at $\theta = \theta_1$ we have

$$e_o(\theta_1) = E_b \tag{59a}$$

$$i_L(\theta_1) = I_s \cos\phi - \frac{E_b}{R} - \frac{E_b}{\omega L}\,(\pi - \theta_1) \tag{59b}$$

We have to solve a differential equation for $e_o(t)$, from 0 to $t_1 = \theta_1/\omega$, and satisfy the initial conditions given by Eqs. 57. We recall that the general solution for the voltage across a parallel RLC circuit is given by

$$e_o(t) = Ae^{-\alpha t}\cos\beta t + Be^{-\alpha t}\sin\beta t + I_s Z\cos(\omega t + \phi - \psi) \tag{60}$$

where $\alpha = 1/(2RC)$; $\beta^2 = \omega_o^2 - \alpha^2$; $\omega_o^2 = 1/LC$; $Z = 1/y = (G^2 + (\omega C - 1/\omega L)^2)^{-1/2}$; $\psi = \arctan R[\omega C - 1/\omega L]$; and A and B are integration constants.

The current in the coil is

$$i_L(t) = \frac{1}{L}\int e_o(t)\,dt$$

Integrating Eq. 60, we obtain

$$i_L(t) = \frac{1}{L}\int Ae^{-\alpha t}\cos\beta t\,dt + \frac{1}{L}\int Be^{-\alpha t}\sin\beta t\,dt + \frac{I_s Z}{L}\int \cos(\omega t + \phi - \psi)\,dt$$

$$i_L(t) = \frac{e^{-\alpha t}}{L(\alpha^2 + \beta^2)}\left[A(-\alpha\cos\beta t + \beta\sin\beta t) - B(\alpha\sin\beta t + \beta\cos\beta t)\right]$$

$$+ \frac{I_s Z}{\omega L}\sin(\omega t + \phi - \psi)$$

Since $\alpha^2 + \beta^2 = \omega_o^2$ and $\omega_o^2 L = 1/C$,

$$i_L(t) = Ce^{-\alpha t}\left[(A\beta - B\alpha)\sin\beta t - (A\alpha + B\beta)\cos\beta t\right] + \frac{I_s Z}{\omega L}\sin(\omega t + \phi - \psi)$$

Using the high-Q approximation, we obtain

$$\frac{\beta^2}{\alpha^2} = \frac{\omega_o^2}{\alpha^2} - 1 = 4Q^2 - 1$$

$$\frac{\beta}{\alpha} = (4Q^2 - 1)^{1/2} \approx 2Q$$

It follows that

$$i_L(t) = C\alpha e^{-\alpha t}\left[(2QA - B)\sin\beta t - (2QB + A)\cos\beta t\right] + \frac{I_s Z}{\omega L}\sin(\omega t + \phi - \psi) \qquad (61)$$

At t = 0, according to Eq. 57a, we have

$$e_o(0) = A + I_s Z\cos(\phi - \psi) = -E_b$$

$$A = -E_b - I_s Z\cos(\phi - \psi) \qquad (62)$$

Again, by Eqs. 57b and 61,

$$i_L(0) = -C\alpha(2QB + A) + \frac{I_s Z}{\omega L}\sin(\phi - \psi) = I_s\cos\phi + \frac{E_b}{R}$$

$$2Q\alpha C\,B = -\alpha AC + \frac{I_s Z}{\omega L}\sin(\phi - \psi) - I_s\cos\phi - \frac{E_b}{R}$$

Since $2\alpha CQ = (2QC)/(2RC) = Q/R$, it follows that

$$B = -\frac{E_b}{2Q} + \frac{I_s Z}{2Q}\cos(\phi-\psi) + \frac{\omega_o}{\omega} I_s Z \sin(\phi-\psi) - \frac{I_s R}{Q}\cos\phi \tag{63}$$

in which we have used Eq. 62. In terms of $\eta = (I_s Z)/(E_b)$, Eqs. 62 and 63 become

$$A = -E_b[1 + \eta\cos(\phi-\psi)] \tag{64}$$

$$B = -\frac{E_b}{2Q}\left[1 - \eta\cos(\phi-\psi) - \frac{2Q\omega_o}{\omega}\sin(\phi-\psi) + \frac{2\eta R}{Z}\cos\phi\right] \tag{65}$$

We now have the complete solution in terms of ϕ. For $t = \theta_1/\omega$, expression 60 yields

$$Ae^{-(\alpha\theta_1)/\omega}\cos\frac{\beta\theta_1}{\omega} + Be^{-(\alpha\theta_1)/\omega}\sin\frac{\beta\theta_1}{\omega} + I_s Z\cos(\theta_1 + \phi - \psi) = E_b \tag{66}$$

Again, by using Eqs. 61 and 59, we have

$$\frac{e^{-(\alpha\theta_1)/\omega}}{2R}\left[(2QA - B)\sin\frac{\beta\theta_1}{\omega} - (2QB + A)\cos\frac{\beta\theta_1}{\omega}\right] + \frac{I_s Z}{L}\sin(\theta_1 + \phi - \psi)$$

$$= -I_s\cos\phi - \frac{E_b}{R} - \frac{E_b}{\omega L}(\pi - \theta_1) \tag{67}$$

Expressions 64-67 give the solution of our problem. This set of equations must be solved to yield θ_1 (and ϕ as a by-product) as a function of η.

These expressions can be further simplified by assuming that we are driving the system close to the resonant frequency. Thus if we let $A = -E_b M$ and $B = -E_b N$, we have $e^{(\alpha\theta_1)/\omega} \approx 1 - (\alpha\theta_1)/\omega$. Since $\alpha/\omega \ll 1$ for a high-Q circuit, $\sin(\beta\theta_1)/\omega \approx \sin\theta_1$; and $\cos(\beta\theta_1)/\omega \approx \cos\theta_1$. Equations 64-67 become

$$\eta\cos(\theta_1 + \phi - \psi) - \left[1 - \frac{\alpha\theta_1}{\omega}\right][M\cos\theta_1 + N\sin\theta_1] = 1 \tag{68}$$

$$-\eta\sin(\theta_1 + \phi - \psi) - \frac{\omega L}{2R}\left[1 - \frac{\alpha\theta_1}{\omega}\right][(N - 2QM)\sin\theta_1 + (M + 2QN)\cos\theta_1]$$

$$-\frac{\omega L}{Z}\eta\cos\phi + \theta_1 = \pi + \frac{\omega L}{R} \tag{69}$$

$$M = 1 + \eta\cos(\phi-\psi) \tag{70}$$

$$N = \frac{1}{2Q}\left[1 - \eta\cos(\phi-\psi) - \frac{2Q\eta\omega_o}{\omega}\sin(\phi-\psi) + \frac{2\eta R}{Z}\cos\phi\right] \tag{71}$$

This is our final result. For simplicity, Eqs. 68-71 will be referred to as the "tuned-limiter equations," or simply as the "limiter equations."

Although they are simplified as much as possible, the limiter equations are still meaningless unless a simple solution is found for the system. We did not find a way out of this situation, and therefore we decided to work out the system for particular values of the variables.

6.3 NUMERICAL SOLUTION OF THE LIMITER EQUATIONS

We have derived a set of equations (Eqs. 68-71) whose solutions should yield the ignition angle θ_1 and the phase angle of the input current ϕ as a function of η. These are the limiter equations. A formal solution of these equations (if it is possible) would seem to be too involved to be of any use. Therefore, our alternative is a numerical solution.

For the elements in the diagram of Fig. 19a, the following values have been chosen: R = 12,500 ohms; $C = 2 \times 10^{-11}$ farads; and $L = 1/72 \times 10^{-3}$ henries. Consequently, $\omega_o = 6 \times 10^7$; Q = 15; and $\alpha = 2 \times 10^6$. The frequency of approximately 10 mc is of common use in FM intermediate-frequency channels. The choice of Q = 15 is dictated by the considerations of section 6.2.

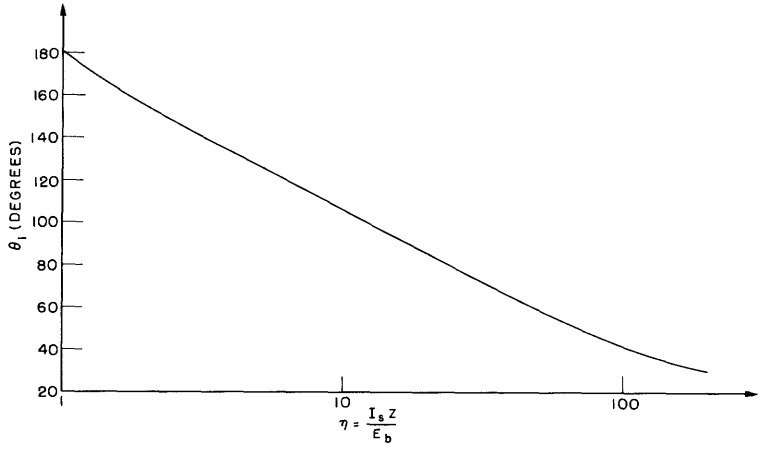

Fig. 20. Ignition angle θ versus driving ratio η.

The numerical results obtained for values of η extending from 1 to 100 are shown in Table 1, for $\omega = 6 \times 10^7$ (limiter driven at center frequency). The values of θ_1 versus η are plotted in Fig. 20. We also find it desirable to solve Eq. 60. Near center frequency, with the high-Q approximation, Eq. 60 becomes

$$e_o(t) = \left[1 - \frac{\alpha\theta}{\omega}\right](A \cos\theta + B \sin\theta) + I_s Z \cos(\theta + \phi - \psi)$$

Letting $M = -A/E_b$, $N = -B/E_b$, and with a center frequency of $\psi = 0$, we find that

$$\frac{e_o}{E_b} = \eta \cos(\theta+\phi) - \left(1 - \frac{\alpha\theta}{\omega}\right)(M \cos\theta + N \sin\theta) \qquad (72)$$

The values of M and N for the solution of Eq. 72 are found by using the auxiliary formulas:

$$M = 1 + v$$

$$N = \frac{1 + v}{30} - u$$

These formulas, as well as those leading to the auxiliary variables u and v, are shown in Table 2, where u and v are listed for several values of θ_1. With the help of these

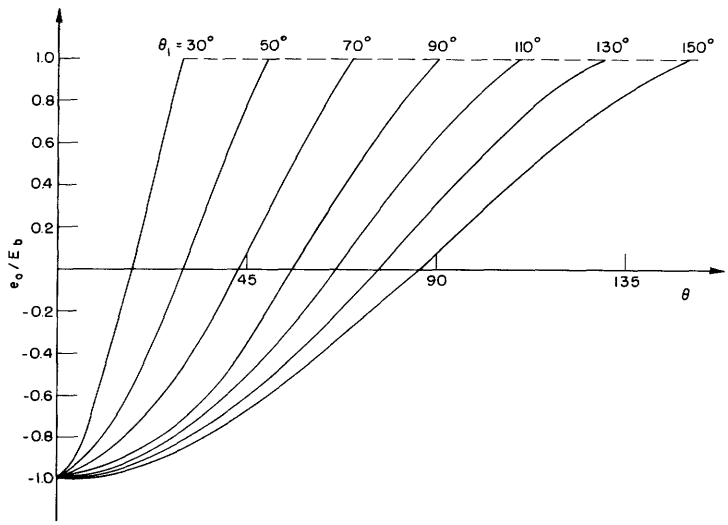

Fig. 21. Variation of zero crossings with ignition angle θ_1.

data, Eq. 72 was solved and plotted in Fig. 21. Actually, only the curves for $\theta_1 = 30°$, 90°, and 150° were plotted from Eq. 68; the other curves were interpolated. The accuracy is not very high except near the zero crossings.

6.4 VALIDITY OF THE RESISTIVE MODEL

We are now in a position to check our earlier assumptions concerning the resistive model. Since we have only a numerical solution for θ_1 (phase considerations were kept out of the resistive model), the obvious procedure is to compare it with the predictions of the resistive theory for the same numerical values. (Notice that the conduction angle θ_1 used here is equal to twice the corresponding θ_1 as defined in Section II.)

The actual solution and the resistive-model solution are shown in Fig. 22a for η = 2.28, and in Fig. 22b for η = 10. The shortening of the conduction periods in the actual solution is apparent. However, the comparison of conduction periods is not fair, since the output of our resistive model is not the flat-topped wave shown in Fig. 22, but its fundamental component.

Accordingly, we have replotted the output voltage $e_o(\theta)$ in Fig. 23, where the fundamental component of the resistive-model output voltage, $A_1(\theta)$, is also shown. The agreement is as reasonable as could be expected between a sinusoidal and a nonsinusoidal

Table 1. Particular solution of the limiter equations.

η	θ_1 (degrees)	ϕ (degrees)
1	180	-180
2	156	-169
5	128	-150
10	106	-135
20	86	-120
30	73	-113
50	60	-106
75	52	-102
100	43	-99

Table 2.

$$\left.\begin{aligned} u &= \eta \sin \phi \\ v &= \eta \cos \phi \end{aligned}\right\} \text{ versus } \theta_1$$

θ_1 (degrees)	u	v
5	-7873.7	-23.21
10	-1964.6	-22.02
30	-211.23	-18.97
50	-73.57	-15.67
70	-30.23	-12.48
90	-14.00	-9.44
110	-6.25	-6.52
130	-2.25	-4.14
150	-0.52	-2.22
170	-0.026	-1.14

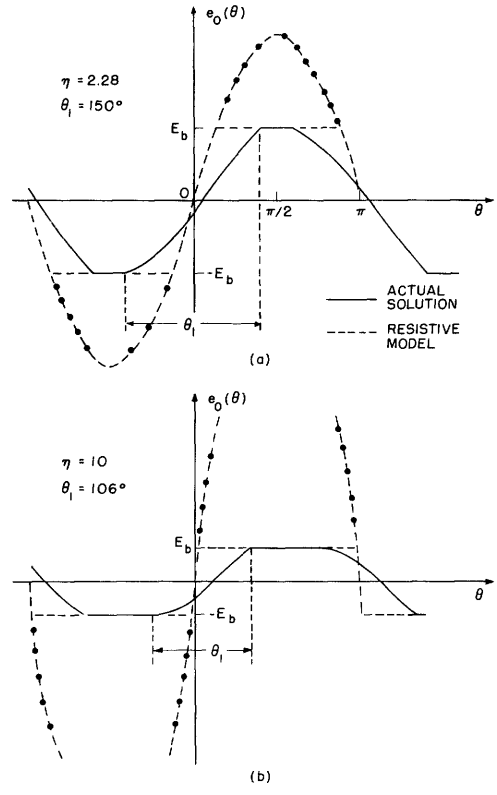

Fig. 22. Output voltage e_o as obtained from the limiter equations and resistive model versus θ.

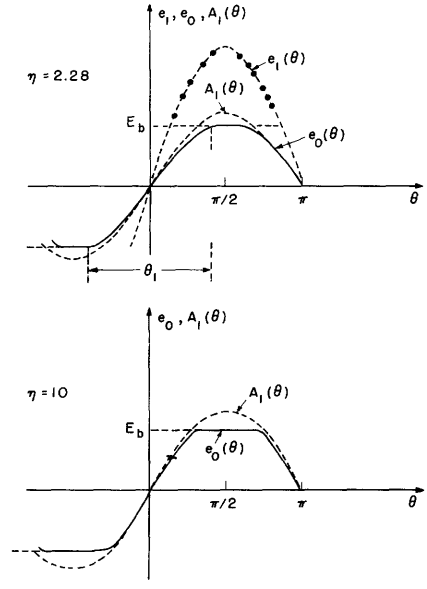

Fig. 23. Typical dependence of the fundamental component of output voltage (A_1) from the resistive model and solution of the limiter equations (e_o) upon θ.

wave. It must be recalled that the solution of the limiter equations would not exhibit a flat top if we had refined our model by introducing square-law diodes as we did in Section IV. This revised solution would improve the agreement between the two waveforms, but we hardly feel that the improvement would be worth the extra labor and time that would have to be employed. The limiter equations look complicated enough as they stand. As a matter of fact, we even feel justified, by the present results, in abandoning the limiter equations altogether. All in all, we are satisfied with the resistive model. We have just shown that it is a good approximation. Furthermore, it is a workable model, which is much more than can be said about the limiter equations.

It is apparent from Fig. 23 that the main discrepancy between $e_o(\theta)$ and $A_1(\theta)$ is in the harmonic content, rather than in the fundamental component. The fact that, thus far, only the fundamental component has been used for the output voltage of the resistive model suggests that this model may be considered as consisting of two independent cascaded circuits: a double-diode clipper shunted by an equivalent resistance, followed by an ideal bandpass filter tuned to the expected center frequency. In Section VII it will be shown that the solution of the limiter equations indicates a phase variation with the driving ratio that was hardly predictable from our previous considerations. Accordingly, a new model for the bandpass filter will be attempted, in order to account for this variation, as well as for the harmonic content.

VII. FREQUENCY DISTORTION IN AMPLITUDE LIMITERS

Heretofore we have concerned ourselves solely with the amplitude of the output voltage of a limiter. The very fact that we chose a resistive model to represent the limiter excluded all considerations of phase.

However, in a practical circuit with tuned elements we would obviously expect a phase variation in the output voltage, with variations in the input signal frequency. Another kind of phase variation has been revealed by the solution of the limiter equations. Numerical results indicate that the phase angle of the output voltage is dependent upon the amplitude of the input current. Since this implies that amplitude modulation can be converted to phase modulation in the limiter, we decided to examine the matter more carefully. The results of this investigation will be the subject of this section.

7.1 PHASE SOLUTION OF THE LIMITER EQUATIONS

Figure 24 shows the input current $i_s(\theta)$, whose phase angle ϕ with respect to the time origin was determined by the solution of the limiter equations. It also shows $e_o(t)$, whose phase angle ϕ_1 (measured from zero crossing to time origin) can be taken from Fig. 21. From inspection of Fig. 24, we can write

$$\phi_2 = \phi_1 - \left[\phi - \frac{\pi}{2}\right]$$

for the phase lag ϕ_2 of $e_o(\theta)$ with respect to $i_s(\theta)$. The $\pi/2$ difference arises from the fact that ϕ is the phase angle of a cosine wave, rather than of a sine wave. Since the phase of the output voltage can only be determined with respect to its zero crossing, the input phase must be converted.

The values of ϕ_2 are listed in Table 3 against the corresponding driving ratios, and

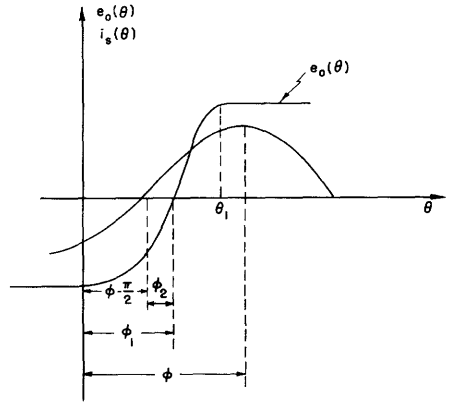

Fig. 24. Typical wave shapes of input current (i_S) and output voltage (e_O) versus time, as obtained from the solution of the limiter equations.

Table 3. Phase lag of the output voltage ϕ_2 as a function of η.

η	$\phi - \pi/2$ (degrees)	ϕ_1 (degrees)	ϕ_2 (degrees)
1	90	90	0
2	79	88	-8
5	60	75	15
10	45	64	19
20	30	52	22
30	23	45	22
50	16	36	20
75	12	29	17
100	9	25	16
200	5	16	11

plotted in Fig. 25. When $\eta = 1$, $\phi_2 = 0$, as expected, for the resonant frequency. As η increases, ϕ_2 increases, reaching a maximum of 22° for values of η between 20 and 30. From then on, ϕ_2 decreases at a slower rate and seems to approach zero again for extremely high driving ratios.

A heuristic explanation can be attempted if we look more closely at the solution of the limiter equations plotted in Fig. 21. We must recognize the fact that the output-voltage waveform, when the diodes are open, is the superposition of a steady-state and a transient component. For a given frequency, the steady-state component has a fixed phase angle. However, the phase angle of the transient component (represented by its first zero crossing) may vary with the damping of the circuit. If we realize that as the driving ratio is increased the loading effect of the diodes increases the damping, we would expect a lowering of the damped resonant frequency, and hence a variation in the phase angle of the transient component. The corresponding variation in the phase angle of the output voltage will depend on the relation between the amplitudes of the steady-state and transient components. This relation is by no means obvious. As a matter of

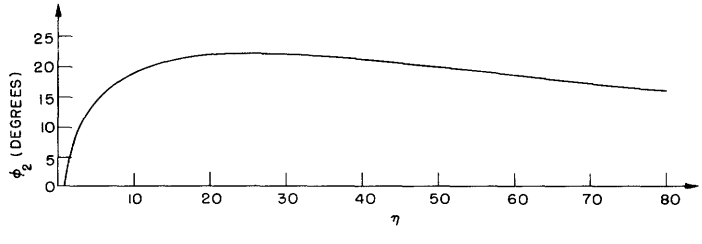

Fig. 25. Phase lag ϕ_2 of $e_o(\theta)$ with respect to $i_s(\theta)$ as a function of the driving ratio η.

fact, the complexity of both the limiter equations and their solutions precludes the practicability of any further investigation in the time domain.

7.2 REVISED VERSION OF THE RESISTIVE MODEL

As we pointed out in section 6.4, the resistive model may be considered as consisting of two independent circuits: a clipper and an ideal filter. We assumed, accordingly, that only the fundamental component would appear at the output of the filter. We shall now admit that the damping caused by the diodes broadens the bandwidth of the tuned circuit. Therefore, part of the higher-order harmonic content of the clipper output will be allowed to pass through the filter. We know that the phase shift of the harmonics varies with the damping of the filter, thereby upsetting the phase angle of the output voltage. We would like to correlate the phase predictions of this revised model with those required by the solution of the limiter equations. Unfortunately, the limiter equations were solved for ideal diodes and a shunt resistance of 12,500 ohms, while the numerical solution of the resistive model implied square-law diodes and a shunt resistance of 6000 ohms. In Section VI, we were able to compare the amplitudes because they depended in both cases upon the driving ratio only. Here, the damping effect must be computed on the basis of the equivalent resistance of the square-law diodes, which depends upon both the driving current and bias rather than on the driving ratio. Although a quantitative correlation is precluded, it is certainly possible to compare the general features of both solutions. This will now be done for the third harmonic of the output voltage.

7.3 EQUIVALENT BANDWIDTH OF THE TUNED CIRCUIT

As a first approximation to the problem of phase shift in the limiter, we shall compute the amount of third harmonic that goes through the filter as damping is increased. From the results of sections 2.3 and 4.2 we can write, for the third-harmonic amplitude,

$$A_3 = \frac{4E_1}{\pi}\left[\frac{\sin 2\theta_1}{2} - \frac{\sin 4\theta_1}{4} + \frac{\sin\theta_1 \cos 3\theta_1}{3}\right]$$

$$+ \frac{4I_s R_L}{\pi}\left[-\frac{\sin 2\theta_1}{2} + \frac{\sin 4\theta_1}{4} + \frac{\sin\theta_1 \cos 3\theta_1}{3}\right]$$

After a few trigonometric transformations, we find that

$$A_3 = \frac{4I_s}{\pi}\left[(R_1 - R_L)(\sin 3\theta_1 \cos\theta_1) + \frac{1}{3}(R_1 + R_L)(\sin\theta_1 \cos 3\theta_1)\right] \tag{73}$$

On the other hand, the impedance of the tuned circuit is

$$Z = \left(G_L^2 + \left[\omega C - \frac{1}{\omega L}\right]^2\right)^{-1/2} \tag{74}$$

with a phase characteristic

$$\phi(Z) = \tan^{-1} R_L\left[\frac{1}{\omega L} - \omega C\right] \tag{75}$$

We shall calculate the impedance to the third harmonic Z_3 and the corresponding phase angle $\phi(Z_3)$ for the tuned circuit used in Section VI, for which the center frequency was 6×10^7 rad/sec. Instead of R, however, we shall use the equivalent resistance R_L calculated in Section V. Table 4 shows the amplitudes of the fundamental and third harmonic calculated by the methods of Section V. A shunt resistance of 6000 ohms and a bias of 4 volts (chosen arbitrarily) were used. These are the amplitudes at the input of the filter. Since we have assumed that the fundamental component goes through the filter unchanged, the output of the third-harmonic component can be found by multiplying the input voltage by Z_3/Z_1, with Z_3, the impedance to the third harmonic, and $Z_1 = R_L$ (at center frequency), the impedance at resonance.

The impedance Z_3 and phase angle $\phi(Z_3)$ were calculated by expressions 71 and 72. In Table 5, Z_3, Z_3/Z_1, $\phi(Z_3)$, and A_{3_o} (the third-harmonic output) are listed against I_s and η. If we examine the amplitudes and phase angles of the third-harmonic component, we notice that for very low driving ratios, the amplitude is small and the phase is maximum. The phase angles decrease steadily with increasing driving ratio, and the amplitudes approach the limiting value of 1.7 volts (input amplitude). Because of the small amplitude at very low driving ratios, we would expect a small phase contribution to the output voltage. On the other hand, for very high driving ratios, the amplitude remains constant, while the phase angles become smaller and smaller. Again, we would expect a negligible phase variation. There is obviously an intermediate region for which the output phase is maximum.

Table 4. Amplitudes of fundamental and third harmonic before filtering.

R_1 = 6000 ohms, E_b = 4 volts		
I_s (ma)	A_1 (volts)	A_3 (volts)
1	4.8	0.045
2	5.3	1.41
5	5.8	1.63
10	6.2	1.7
15	6.4	1.7
20	6.6	1.7
30	7.0	1.7
40	7.2	1.7

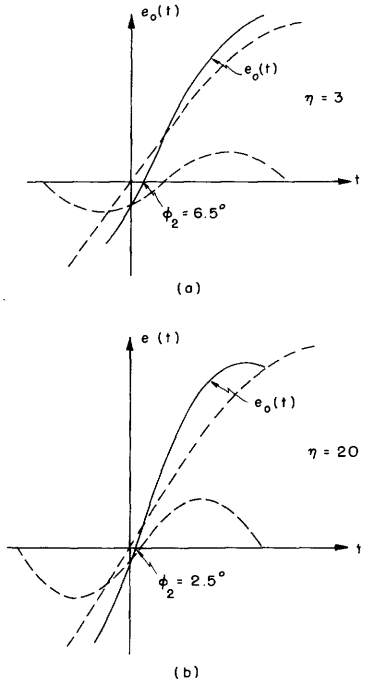

Fig. 26. Phase angle ϕ_2 contributed by the third harmonic of the output voltage.

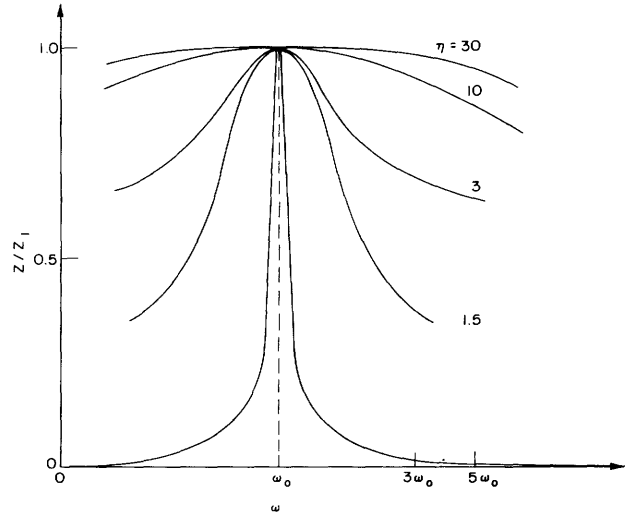

Fig. 27. Frequency response of the tuned limiter.

Table 5. Amplitude and phase of the third-harmonic component at the output of the filter.

I_s (ma)	η	R_D (ohms)	R_L (ohms)	Z_3 (ohms)	Z_3/Z_1	$\phi(Z_3)$ (degrees)	A_{3_o} (volts)
1	1.5	900	780	295	0.38	22.7	0.017
2	3	350	330	224	0.68	15.3	0.96
5	7.5	170	165	145	0.88	9.3	1.44
10	15	115	112	106	0.94	6.6	1.6
15	22.5	95	93.5	89	0.95	5.5	1.62
20	30	80	79	77	0.975	4.8	1.66
30	45	64	63	62	0.985	3.8	1.68
40	60	55	54.5	54	0.99	3.3	1.69

As a rough check on these expectations, for $\eta = 1.5$, although $\phi(Z_3) = 22.7°$, the amplitude $A_{3_o} = 0.017$, less than 0.5 per cent of the fundamental $A_1 = 4.8$. The phase angle is very close to zero. For $\eta = 3$, Fig. 26a shows that the resultant phase ϕ_2 equals 6.5°. For $\eta = 20$, Fig. 26b shows that ϕ_2 drops to 2.5°.

Therefore, although numerical values are widely different, the general features of this solution agree with the solution of the limiter equations. It is apparent that the phase variations would increase if we took into consideration the other higher-order harmonics.

Considering these results, we can feel reasonably sure that the damping introduced by the diodes broadens the bandwidth of the tuned circuit. A rough sketch is shown in Fig. 27 where, for a few representative values of η, the response of the tuned circuit is plotted as a function of frequency. It is apparent that, as soon as the diodes begin to conduct, the bandwidth becomes a function of the driving ratio, and so does the higher-harmonic content in the output voltage.

The solutions of the limiter equations, and of the modified version of the resistive model indicate that there is a conversion of amplitude-to-phase modulation in the limiter. However, a glance at Fig. 25 shows that this effect might not be easily detectable, except for low driving ratios.

VIII. CONCLUSION

The results of this report have shed some light on the more elementary aspects of our problem. In particular, we feel that the following issues have been settled:

(i) The output waveform of the double-diode limiter is nonsinusoidal, except for very low driving ratios. Both the solutions of the limiter equations and experimental evidence (10) lead to this conclusion.

(ii) The resistive model with square-law diodes is a good first approximation for an actual limiter, as far as magnitudes are concerned.

(iii) The mutual interaction between the diodes and the tuned circuit may be accounted for, as a first approximation, by assuming that the equivalent resistance of the diodes shunts the tuned circuit, thereby widening its bandwidth.

If the resistive model is accepted as a reasonable approximation, all the conclusions of Section V are valid. In particular, we would like to suggest the use of the limiter coefficient K_L as a representative parameter for the design of limiters. It is also strongly suggested that some experimental work be carried out along these lines. For instance, the limiter coefficient should be calculated for a few representative types of diode, and the reduction in modulation measured for several values of bias, shunt resistance, driving current, and percentage of modulation. A practical method of measuring the limiter coefficient is also desirable, so that charts can be issued by manufacturers specifically for the use of limiter designers. Finally, the optimization of limiter design with respect to maximum expected modulation, gain-bandwidth product, number of stages, and value of bias is a problem that suggests itself. Suffice it to say that the actual design of limiters is still being carried out on an empirical basis. The phase distortion predicted by the solution of the limiter equations is probably one of the most important aspects of the problem. It would be an interesting project to set up a controlled experiment in which all of the remaining causes of distortion would be absent, leaving the distortion to be introduced by whatever limiting process is in evidence.

Acknowledgment

The author wishes to express his gratitude to Professor Elie J. Baghdady, without whose invaluable assistance and encouragement this research could not have been carried out.

References

1. J. Granlund, Interference in frequency-modulation reception, Technical Report 42, Research Laboratory of Electronics, M.I.T., Jan. 20, 1949.
2. E. P. Brandeau, Analysis of a broad band FM limiter, S.M. Thesis, Department of Electrical Engineering, M.I.T., 1950.
3. D. L. Shapiro, Analysis of diode limiter, S.B. Thesis, Department of Electrical Engineering, M.I.T., 1941.
4. R. Paananen, IF and detector design for FM (Parts 1-3), TV Rad. Eng., Vol. 23, No. 2, p. 20 (April-May 1953); No. 3, p. 21 (June-July 1953); No. 4, p. 18 (Aug.-Sept. 1953).
5. J. Granlund, op. cit., p. 15.
6. T. S. Gray, Applied Electronics (John Wiley and Sons, Inc., New York, 1955).
7. F. E. Terman, Electronic and Radio Engineering (McGraw-Hill Publishing Company, Inc., New York, 1955).
8. E. J. Baghdady, Interference rejection in FM receivers, Technical Report 252, Research Laboratory of Electronics, M.I.T., Sept. 24, 1956.
9. R. Madsen, Amplitude to phase conversion in clipper limiters, Technical Memorandum 54-212-44, Bell Telephone Laboratories, Inc., New York, 1954.
10. P. M. Lally and A. T. Raczynski, A study of the limiting properties of two devices: A. Germanium crystals; B. Cathode coupled amplifiers, S.B. Thesis, Department of Electrical Engineering, M.I.T., 1948.